T.R.N.C.

NEAR EAST UNIVERSITY

INSTITUTE OF HEALTH SCIENCES

THE EFFECT OF AMITRIPTYLINE ON EQUINE SERUM BUTYRYLCHOLINESTERASE: KINETIC STUDIES AND DOCKING CALCULATIONS

Sani Muhammad UZAIRU

MEDICAL BIOCHEMISTRY PROGRAM

MASTER OF SCIENCE THESIS

NICOSIA

2017

T.R.N.C.

NEAR EAST UNIVERSITY

INSTITUTE OF HEALTH SCIENCES

THE EFFECT OF AMITRIPTYLINE ON EQUINE SERUM BUTYRYLCHOLINESTERASE: KINETIC STUDIES AND DOCKING CALCULATIONS

Sani Muhammad UZAIRU

MEDICAL BIOCHEMISTRY PROGRAM

MASTER OF SCIENCE THESIS

SUPERVISOR

Asst. Prof. Dr. Kerem TERALI, PhD

NICOSIA

2017

The Directorate of Health Sciences Institute,

This study has been accepted by the Thesis Committee in Medical Biochemistry Program as a Master of Science Thesis.

Thesis committee:

Chair:	Professor Nazmi ÖZER, PhD Near East University
Supervisor:	Assistant Professor Kerem TERALI, PhD Near East University
Member:	Professor Naciye Leyla AÇAN, PhD Hacettepe University

Approval:

According to the relevant articles of the Near East University Postgraduate study-Education and Examination Regulations, this thesis has been approved by the above mentioned members of the thesis committee and the decision of the Board of Directors of the institute.

Professor K. Hünsü Can BAŞER, PhD
Director of Graduate School of Health Sciences

DECLARATION

I hereby declare that the work in this thesis entitled "**THE EFFECT OF AMITRIPTYLINE ON EQUINE SERUM BUTYRYLCHOLINESTERASE: KINETIC STUDIES AND DOCKING CALCULATIONS"** is the product of my own research efforts undertaken under the supervision of Assistant Professor Kerem Terali. No part of this thesis was previously presented for another degree or diploma in any university elsewhere, and all information in this document has been obtained and presented in accordance with academic ethical conduct and rules. All materials and results that are not original to this work have been duly acknowledged, fully cited and referenced.

Name, Last Name:

Signature:

Date:

ACKNOWLEDGEMENT

Utmost gratitude goes to Almighty Allah. And without further ado, some special mention has to be made of Prof. (Dr.) Nazmi Özer (Chair: Department of Medical Biochemistry), Prof. (Dr.) Hamdi Ogus, Assoc. Prof. (Dr.) Özlem Dalmizrak and ultimately, my supervisor, Asst. Prof. (Dr.) Kerem Terali for their generous contributions towards the success of this work.

Asst. Prof. (Dr.) Kerem Terali particularly has been of tremendous resourcefulness and support.

Equally deserving of gratitude is Dr. Abubakar Labaran Yusuf, BMBch, FCMP, as well as the duo of Professor Muhammad Atiku Kano and Professor Alhassan Muhammad Wudil who groomed me whilst at Bayero University, Kano as an undergraduate student.

Worthy of note also is my single mother who defied financial odds to support my education up to the secondary school level, from where a string of scholarships brought me this far.

Finally, I wish to express my indebtedness to my laboratory colleague, Qendresa Hotti, and everyone that bought into and supported my vision to pursue M.Sc.

ABSTRACT

Uzairu S.M. The Effect of Amitriptyline on Equine Serum Butyrylcholinesterase: Kinetic Studies and Docking Calculations. Near East University, Institute of Health Sciences, Medical Biochemistry Program, M.Sc. Thesis, Nicosia, 2017.

Butyrylcholinesterase, a serine hydrolase, is an important detoxification enzyme with unique roles in cholinergic function. In this study, the effect of amitriptyline on the hydrolysis of butyrylthiocholine by butyrycholinesterase, purified from equine serum, was investigated using kinetic and molecular docking procedures. Amitriptyline (0.244 µM – 125 µM) inhibited the activity of butyrylcholinesterase in a dose dependent fashion with an IC_{50} of 10 µM. Lineweaver–Burk plot and the secondary replots of Dixon revealed a linear mixed-type inhibition with a predominantly competitive nature. The inhibitory rate constant, $K_{i,}$ was 2.25 ± 0.66 µM whilst the V_m and α were found to be 1070 ± 28 U mg^{-1} protein, and 7.34 ± 1 µM, respectively. Analysis of kinetic constants showed that amitriptyline triggered more than 3-fold decline in butyrylcholinesterase's affinity for butyrylthiocholine. This is even as the K_s was discovered to have rose from 0.169 ±0.019 to 0.551±0.028 mM. Amino acid sequence alignment of equine and human serum butyrylcholinesterase indicated a 90.4% sequence identity. Docking study revealed that the Phe329 and Trp231 of the lowest energy cluster established an effective л–л stacking with the aryl moiety of amitriptyline. The subtle noncompetitive component was discovered to have resulted from an electrostatic interaction (salt bridge) between amitriptyline and Asp70 of the peripheral anionic residue. Amyloid beta peptides are presumed to deposit at the peripheral anionic site, hence a target in anti-AD therapy. Taken together, amitriptyline exerted strong inhibitory potency against butyrylcholinesterase slightly above therapeutic doses; and hence, could be optimized for therapeutic utility in Alzheimer disease.

Keywords: amitriptyline, butyrylcholinesterase, linear mixed type inhibition, Alzheimer disease

ÖZET

Uzairu S.M. At Serum Butirilkolinesteraz Amitriptilinin Etkisi: Kinetik Araştırmalar ve Doklama Hesaplamaları. Yakın Doğu Üniversitesi, Sağlık Bilimleri Enstitüsü, Tıbbi Biyokimya Programı, Yüksek Lisans Tez, Lefkoşa, 2017.

Butilklolinesteraz, serin hidrolaz, kolinerjik fonksiyonda eşsiz rolü olan önemli bir detoksifikasyon enzimidir. Bu çalışmada, at serumundan arıtılmış butirilkolinesteraz ile butiriltiokolin hidrolizi üzerine amitriptilinin kinetik ve moleküler yerleştirme yöntemleri üzerindeki etkisi araştırılmıştır. Amitriptilin (0.244 μM - 125 uM), butirilkolinesteraz'ın aktivitesini 10 uM IC_{50} ile doz bağımlı bir tarzda inhibe etti. Lineweaver-Burk ve Dixon'ın ikincil replotları ağırlıklı olarak rekabetçi nitelikte doğrusal bir karışık tip inhibisyonu ortaya koydu. Engel hız sabiti K_i, 2.25 ± 0.66 μM iken, V_m ve α'nın sırasıyla 1070 ± 28 U mg^{-1} protein ve 7.34 ± 1 μM olduğu bulunmuştur. Kinetik sabitlerin analizi amitriptilinin butirilkolinesterazın bütiriltiokolin için olan afinitesinde 3 kattan fazla bir düşüşe neden olduğunu gösterdi. Bu, K_s'nin 0.169 ± 0.019'dan 0.551 ± 0.028 mM'ye yükselmesi ile sonuçlanmiştir. At ve insan serum butirilkolinesterazının amino asit dizilimleri,% 90.4'lük bir dizi benzerliği gösterdi. Takma çalışması, en düşük enerji kümelenmesinin Phe329 ve Trp231'inin amitriptilinin aril kısmı ile etkili bir л-л istifleme oluşturduğunu ortaya koymuştur. Hafif rekabetçi olmayan bileşenin, periferik anyonik kalıntıya ait amitriptilin ve Asp70 arasındaki bir elektrostatik etkileşimden (tuz köprüsü) kaynaklandığı keşfedilmiştir. Amiloid beta peptitlerin periferik anyonik bölgede çökeldiği ve dolayısıyla anti-AD terapisinde bir hedef olduğu varsayılmaktadır. Bu bulgular birlikte ele alındığında, amitriptilin, butirilkolinesteraz'a karşı terapötik dozların birazcık üstünde güçlü inhibisyon potensiyeli sergilediği gözlendi; Ve dolayısıyla, Alzheimer hastalığında terapötik kullanım için optimize edilebileceği düşülebilir.

Anahtar Kelimeler: amitriptilin, bütirilkolinesteraz, lineer karışık tip inhibisyonu, Alzheimer hastalığı

TABLE OF CONTENTS

SYMBOLS AND ABBREVIATIONS

A:	Adenine
Aβ:	Beta Amyloid
ABCBAI:	P-glycoprotein
ABP:	Acyl Binding Pocket
ACh:	Acetylcholine
AChE:	Acetylcholinesterase
AD:	Alzheimer Disease
AMI:	Amitriptyline
APP:	Amyloid Precursor Protein
AS:	Acylation Site
Asp:	Aspartate
BChE:	Butyrylcholinesterase
BTCh:	Butyrylthiocholine
C:	Cytosine
CBS:	Choline Binding Site
Ch:	Choline
ChAT:	Choline Acetyltransferase
ChE:	Cholinesterase
CNS:	Central Nervous System
CYP3A4:	Cytochrome P450 34
CYP2C19:	Cytochrome P450 2C19
CYP2D6:	Cytochrome P450 2D6
dH_20:	Distilled Water
DTNB:	$5,5^I$ dithiobis (2-nitrobenzoic Acid)
E:	Glutamine
EqBChE:	Equine Butyrylcholinesterase
G:	Guanine
F:	Phenylalanine
$GABA_A$:	γ- aminobutyric Acid type A

Glu:	Glutamine
huAChE:	Human Acetylcholinesterase
huBChE:	Human Butyrylcholinesterase
His:	Histidine
IC_{50}:	Half maximal Inhibitory Concentration
K^+:	Potassium
K_{cat}:	Turnover Number
kDa:	Kilo Dalton
$K_{i:}$	Inhibition Constant
K_m:	Substrate Concentration at Half maximal Velocity
K_s:	Dissociation Constant for Enzyme-Substrate Complex
KOH:	Potassium Hydroxide
Leu:	Leucine
MOPS:	3-(N-morpholino) Propane Sulfonic Acid
mRNA:	Messenger RNA
Na^+:	Sodium
NaF:	Sodium Flouride
NOR:	Nortriptyline
PAS:	Peripheral Anionic Site
PDB:	Protein Data Bank
Phe:	Phenylalanine
PLIP:	Protein Ligand Interaction Profiler
sAPP:	Soluble Amyloid Precursor Protein
Ser:	Serine
SSRI:	Selective Serotonergic
T:	Thymine
TCA:	Tricyclic Antidepressant
TcAChE:	*Torpedo carlifornica* Acetylcholinesterase
TCh:	Thiocholine
TNFα:	Glutamate NMDA Receptor
Trp:	Tryptophan

Tyr:	Tyrosine
Val:	Valine
*V*m:	Maximum Velocity
W:	Tryptophan
Y:	Tyrosine
5-HT_2:	5 hydroxytryptamine receptors

LIST OF FIGURES

LIST OF TABLES

1. INTRODUCTION

The World Health Organization (WHO) 2016 estimates put the prevalence of dementia at 47.5 million people worldwide. Fifty eight percent of these live in low and middle income countries and the projections are that the proportion will shoot up to 71% by 2050. Overall, 135 million people would have suffered dementia by 2050, the report said; and, further stated that 60%–70% of these cases would have been caused by Alzheimer disease (AD), the most common neurodegenerative disease.

Alzheimer disease is triggered by a progressive depletion of the neurotransmitter acetylcholine (ACh) as a result of impaired activity of choline acetyltransferase (ChAT) due to the significant loss of cholinergic neurons culminating in cognitive impairment and memory loss (Mucke, 2009). Therefore, the cholinergic hypothesis, which propounded that there is a material attenuation of cholinergic function in the brain of AD patients, forms the nucleus upon which AD therapy is based. The approach is to restore the pool of the cholinergic neurotransmitter acetylcholine through the use of reversible cholinesterase inhibitors (Hitzeman, 2006).

Cholinesterase is broadly divided into acetylcholinesterase (AChE; EC: 3.1.1.7) and butyrylcholinesterase (BChE; EC: 3.1.1.8). AChE is responsible for hydrolytic breakdown of acetylcholine, and its inhibition has been validated as an efficient way to lessen some behavioral and cognitive system disorders of AD (Citron, 2010). Presently, AChE inhibitors like donepezil, galantamine, tacrine have been utilized for clinical treatment of AD even though their effect is essentially palliative than curative (Shaikh *et al.,* 2014). Besides, their clinical effectiveness is limited by their deleterious side effect on the liver and the peripheral nervous system in addition to their poor bioavailability and selectivity (Toda *et al.,* 2010). These, more than anything, underscore the need to beam the searchlight on butyrylcholinesterase.

Butyrylcholinesterase is a tetrameric enzyme. Its monomers are arranged as a dimer of dimers. Each dimer contains identical monomers linked by inter-chain disulfide bridge (Lockridge *et al*., 1979). Each of the catalytic subunits of this homo tetramer has 574 amino acid residues. It consists of a catalytic triad made up of serine 198, glutamic acid

325 and histidine 438 (Lockridge *et al.,* 1987). Aside the catalytic triad, the active site gorge has an anionic site which can bond to the positively charged quaternary nitrogen of the choline. The anionic site contains tryptophan 82. Three crucial aromatic amino acids found in the peripheral anionic site (PAS) of AChE (Tyr 70, Tyr 121 and Trp 279) are absent at the entrance of the active site gorge of BChE. For this reason, it is at times speculated that BChE has no PAS, at least not one identical to AChE PAS (Masson *et al.,* 2009). Cationic substrates are guided into the active site gorge by communication with tyrosine 332 and aspartic acid 70 which are found at the entrance of the gorge (Velom *et al.,* 1993; Soreq and Seidman, 2001). In BChE, lysine 286 and valine 288 line the acyl pocket within the gorge and this is where the acyl groups are held during catalysis (Velom *et al.,* 1993).

BChE catalyzes the hydrolytic cleavage of butyrylcholine, acetylcholine, succinylcholine etc. It also degrades esters of choline such as cocaine, heroin as well as scavenges anticholinesterase (Lockridge *et al.*, 1980; Galey, 1991; Masson, 1998). Curiously, whilst the biochemical features of BChE are altered in AD, a significant amplification of its activity has been noted. Research has revealed that the surge in the activity of BChE plays a major role in amyloid beta (Aβ) aggregation in the early phases of senile plaque formation (Anand and Singh, 2013). Given that BChE can also hydrolyze acetylcholine, its inhibition might result in further advancement of cholinergic transmission. Consequently, therapeutic candidates that could inhibit BChE could provide a novel benefit and add value in AD treatment (Sim, 1999; Giacobini, 2000).

And this serves the bases for screening the inhibitory activity of the tricyclic antidepressant, amitriptyline (AMI) against purified BChE. AMI is a selective serotonergic re-uptake inhibitor (SSRI). It is degraded into nortriptyline which might complement its effectiveness on norepinephrine re-uptake (Breyer-Pfaff, 2004). Merry (1997) observed that AMI raised the expression of brain derived neurotrophic factor and B-cell lymphoma 2 both of which possess neuroprotective effect. And in the central nervous system of mammals, it enhanced neuronal regeneration (Chen *et al.,* 1997). According to Hu *et al.* (2003), the level of copper, zinc superoxide dismutase is increased by AMI, and this serves a neuroprotective effect in the brain hippocampus.

There are reports in the literature suggesting that antidepressants inhibit cholinesterase (Ahmed *et al*., 2008; Muller *et al.*, 2002). Whilst Barcellos *et al.* (1998) epitomized that imipramine and diazepam but not AMI inhibited AChE from the cerebral cortex of adult rats *in vitro*, Nunes-Tavares *et al.* (2002) observed that AMI inhibits purified AChE from *Electrophorous electricus* (the electric eel) through an interaction at its peripheral anionic site. But most significantly, Cokugras and Tezcan (1997) speculated that AMI inhibits serum BChE by either binding to its putative anionic site or possibly through an interaction with the hydrophobic pocket near its active site; yet fell short of unravelling how the inhibitor docks into either of those sites; and consequently, the veracity of such a proposition requires validation.

Besides the fact that the kinetic behavior of purified BChE in the presence of AMI remains unclear, their molecular mechanism of interaction is also unknown; and even yet, how this interaction equally impacts on the cholinergic system exist only in the realms of conjecture. And by virtue of the forgoing, the kinetic and molecular docking studies of purified BChE with AMI become a fascinating subject to investigate, in the interest of identifying viable therapeutic alternatives for AD treatment. Given the aforementioned prerogatives therefore, the objectives of this study are to:

a. screen and evaluate the inhibitory action of AMI against BChE
b. identify the kinetic mechanism of the inhibition and compute kinetic parameters
c. elucidate the structural features and molecular bases for their binding as well as interaction
d. relate the molecular interaction of AMI and BChE with the cholinergic system

2. GENERAL INFORMATION

2.1. Cholinesterases

Cholinesterases are classified under the protein family called serine hydrolases (P family). This is due to their ability to utilize their catalytic site's serine residue, a nucleophile, to hydrolyze substrates. Cholinesterases have been distinguished into two basic groups, viz.: acetylcholinesterase (AChE; EC: 3.1.1.7) and butyrylcholinesterase (BChE; EC: 3.1.1.8). The former catalyzes the hydrolytic breakdown of its primary substrate, acetylcholine into choline and acetate; whilst the latter, with its broad specificity catalyzes the hydrolytic cleavage of acylcholines to choline and a weak acid. AChE also catalyzes the transacetylation of variety of acetic esters (Silman and Sussman, 2005). The grounds for this division hinges primarily on their specificities for their natural substrates, inhibitors, tissue distribution and kinetic properties (Mesulam *et al.*, 2002). The serine hydrolase super family consists of myriad proteins involved in diverse physiological actions, including blood clotting (Flemmig and Melzig, 2012), digestion (Whitcomb and Lowe, 2007) and most significantly neurotransmission (Pohanka, 2011). Even strikingly, many of these cholinesterases have been implicated in pathological conditions, ranging from pancreatitis, thrombosis to AD (Pohanka, 2011; Flemmig and Melzig, 2012). And in view of the aforesaid, the focus has therefore shifted to cholinesterases as valid and prime targets in drug discovery. It is therefore not surprising that the inhibitors of these enzymes have been used in the therapy of myansthenia gravis (Mehndiratta *et al.*, 2011) and AD (Birks, 2006). Today, drugs like Exelon® (Novartis) for AD; Xarelto® (Bayer) for thrombosis and Onglyza® (Bristol-Myers Squibb) for type 2 diabetes have been developed from the inhibitors of this enzyme superfamily (Bachovchin and Cravatt, 2012).

2.2. Acetylcholinesterase

AChE is viewed as the key enzyme in the cholinesterase family. A serine hydrolase, AChE is affiliated to the α/β hydrolase family (Nardini and Dijkstra, 1999). Getman *et al.* detailed that AChE is encoded by a single gene located on the long arm of chromosome 7 at position 7q22. AChE has narrow substrate specificity and acts classically on its physiological substrate, acetylcholine (ACh) (Getman *et al.*, 1992).

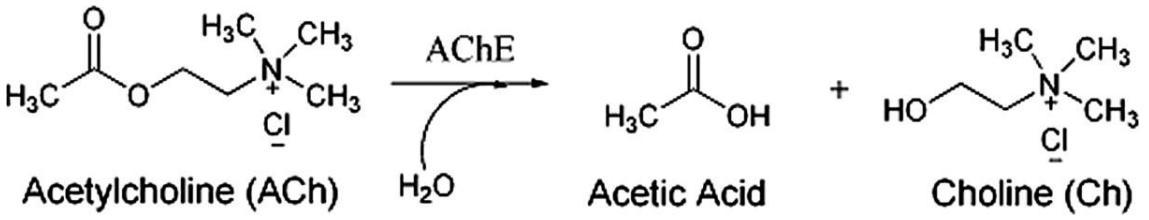

Figure 2.1. Acetylcholinesterase hydrolyzes acetylcholine into acetic acid and choline. Adapted from Xu *et al.* (2008).

The crucial role AChE plays in nerve impulse by hydrolyzing the neurotransmitter acetylcholine and terminating its actions in cholinergic system is well documented. This notwithstanding, suggestions abound of its role as an adhesion protein in synaptic development and maintenance (Munoz-Muriedas *et al.*, 2004); and in addition, evidence of its involvement in neurite growth are beginning to surface (Sharma *et al.*, 2001). AChE has also been figured in the promotion of pathological cluster of amyloid peptide into amyloid fibrils *in vitro* (Bartolini *et al.*, 2003) and *in vivo* (Rees *et al.*, 2003) with complexes of AChE and beta amyloid (Aβ) displaying acute neurotoxicity in relation to fibrils formed by Aβ alone (Reyes *et al.*, 2004).

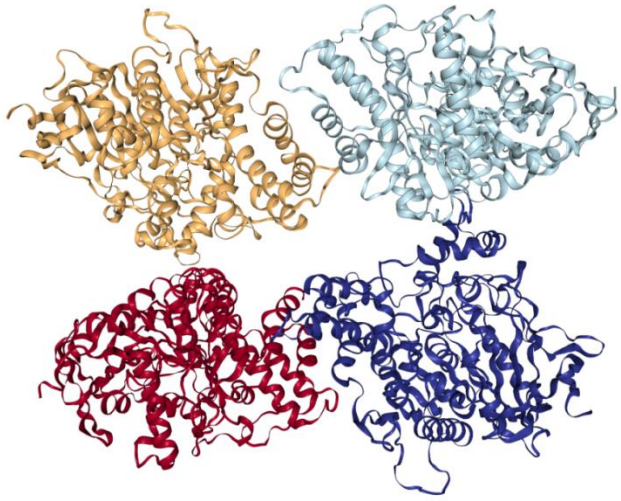

Figure 2.2. Crystallographic assembly of *Electrophorous electricus* acetylcholinesterase tetramer (AChE; PDB ID: 1C2O). Modified from Bourne *et al.* (1999).

2.3. Butyrylcholinesterase

BChE is a serine esterase that is predominant in the plasma and tissues of higher vertebrates where it hydrolyzes a wide range of substrates. These substrates include but not limited to acetylcholine, butyrylcholine and succinylcholine (Ringvold, 2005). BChE has been severally referred to as non-specific choline esterase, pseudocholinesterase, acylcholine acylhydrolase and choline esterase II (Asojo *et al.,* 2011). Liston *et al.* reported that BChE in contrast to AChE is highly active in the peripheral tissues as against the brain (Liston *et al.*, 2004). Also found in the neurons, it is however prevalent in serum and glial cells (Darvesh and Hopkins, 2003). BChE has been linked to various physiological processes like the hydrolysis of choline and non-choline esters such as succinylcholine (Kaufman *et al.,* 2011), acetylcholine (Mesulam *et al.,* 2002), aspirin (Masson *et al.,* 1998) and cocaine (Xue *et al.,* 2011), hence playing an important role in anesthesia, neurotransmission and drug abuse.

More so, BChE has huge pharmacological and toxicological significance. This is informed not only by its ability to hydrolytically cleave ester containing drugs as hinted in the preceding paragraph; but also, by its capacity to serve as scavenger for ChE inhibitors like potent organophosphorous nerve agents, just before they arrive at their synaptic targets (Raveh *et al*., 1997).

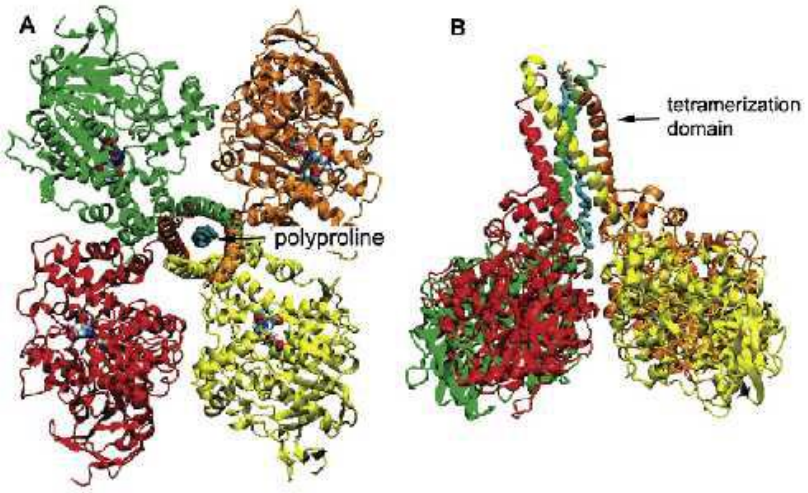

Figure 2.3. Human butyrylcholinesterase tetramer. Adapted from Lockridge O. (2015).

2.3.1. Molecular Structure of Butylrylcholinesterase

A tetramer of four identical subunits, human BChE is a siaglycoprotein of 340 kDa molecular weight. Each monomer has 574 amino acids and 9 linked asparagine complexed glycans. The 198th residue from the amino terminal end is the active site serine. The substrate binding sites of this enzyme protein consist of a peripheral anionic site and a catalytic active site located deep inside a 20 Å gorge. Eight half-cystine is contained in each subunit of the 574 amino acids of human BChE. Three internal disulphide bridges are formed by six of these half-cystine viz.: cys65_cys92; cys252_cys263 and cys400_cys519 (Lockridge *et al.*, 1987).

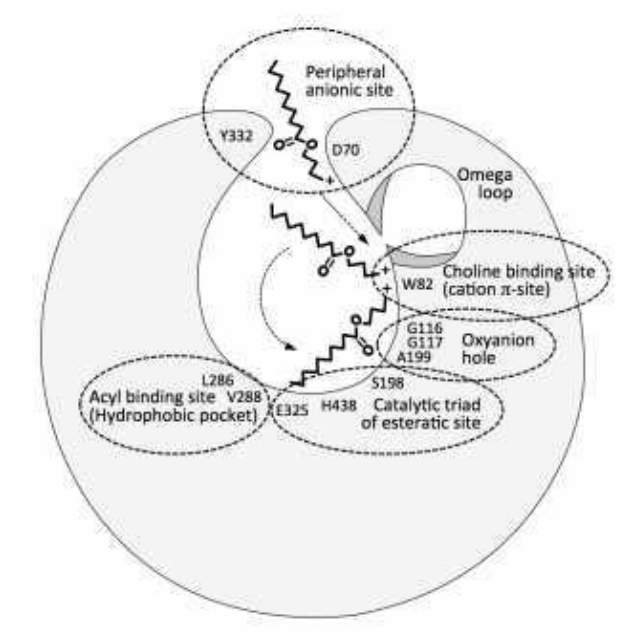

Figure 2.4. Binding sites of BChE monomer. Adapted from Cokugras (2003).

This sialoglycoprotein has a sugar content of 24% by weight. The polypeptide chain has a molecular weight of 65.1 kDa, however as a result of glycosylation it reaches to about 85 kDa on deactivating polyacrylamide gel electrophoresis. The higher amount of glycosylation of BChE is responsible for its longer half-life (Nachon *et al.*, 2002).

Human BChE is encoded by an autosomal gene located on the long arm of chromosome 3 at position 3q26.1_q26.2 (Allderdice *et al.*, 1991). The *BCHE* gene is approximately 73 kb in length, and consists of 1,722 base pairs of coding sequence and four exons.

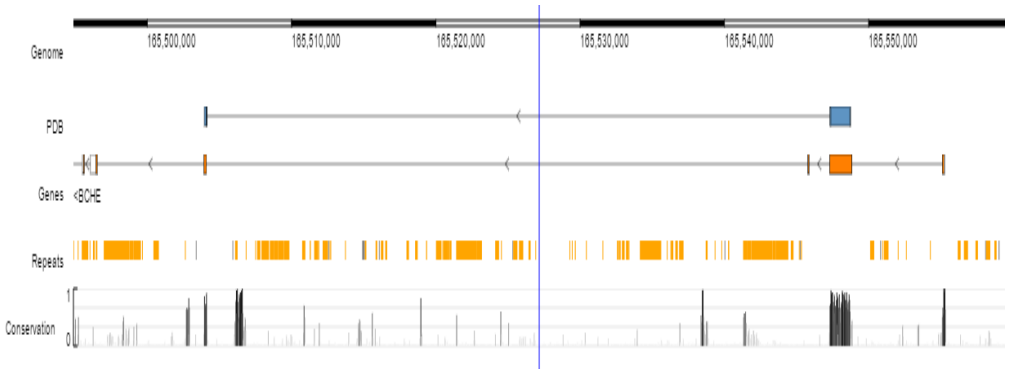

Figure 2.5. BCHE gene organization: Chromosome Location: chr3: 165,491,169-165,548,821; the *genome* is the ruler that shows the nucleotide graphic coding for each nucleotide. The *gene* represents the gene-structure on the genome, white boxes represent the UTRs (untranslated regions) whilst the black lines connecting boxes represent introns. Repeats show various repeat regions that have been annotated along the genome (A: green, T: red, G: yellow, C: blue). Cytogenetic location: 3q26.1; Length coding sequence: 1806 nucleotides**.** Retrieved from http://www.rcsb.org/pdb/gene/BCHE, accessed 17-04-2017.

Exon 1 has untranslated sequences and two possible translation initiation domains at codons 69 and 47. Exon 2 (1,525 base pairs) comprises 83% of the coding sequence for mature protein and a third potential translation initiation at codon 28. Exon 3 is about 167 nucleotides in length, whilst exon 4 consisting of 604 base pairs codes for the carboxyl terminal end of the protein and the 3^{I} untranslated segment where two polyadenylation signals have been discovered. Whilst intron 1 is about 6.5 kb long, the estimated minimum sizes of introns 2 and 3 are about 32 kb each (Arpagaus, 1990).

2.3.2. Differences in the Active Sites of Human Cholinesterases

Even though AChE and BChE are products of distinct genes located on chromosomes 7 and 3 in human, they exhibit 65% homology in their amino acid sequence (Giancobini, 2004). AChE is considered to be the ancestral ChE in vertebrates (Chatonnet and Lockridge, 1989). Additionally, Chatonnet and Lockridge (1989) posited that an early gene duplication incident and its concomitant divergent structural and functional evolution engendered the acetylcholinesterase and butyrylcholinesterase of higher vertebrates. AChE contains a catalytic triad that consist of amino acids serine, histidine and glutamic

acid located beneath the 20 Å gorge as seen through the X ray crystal structures of *Torpedo californica* (Pacific electric ray) (Dvir *et al.*, 2010). This catalytic triad is similar to that in human BChE (Nicolet *et al.*, 2003). The amino acid residues lining this gorge apparently dictate the substrate selectivity as the entry to AChE is narrower when compared with BChE (Fig. 2.6). This is primarily as a result of the aromatic amino acid units Tyr124 and Trp286 located at the entrance of the gorge and occupied by Gln119 and Ala277 in BChE. Inside the gorge, while BChE has smaller amino acid residues Leu286 and Val288 at its acyl binding site, AChE contains Phe288 and Phe290 (Nicolet *et al*., 2003). This difference in acyl binding site residues allows BChE to bind bulkier substrates into its catalytic site. Also, Tyr337 in AChE (Ala328 in BChE) prevents substrates from associating with the catalytic triad.

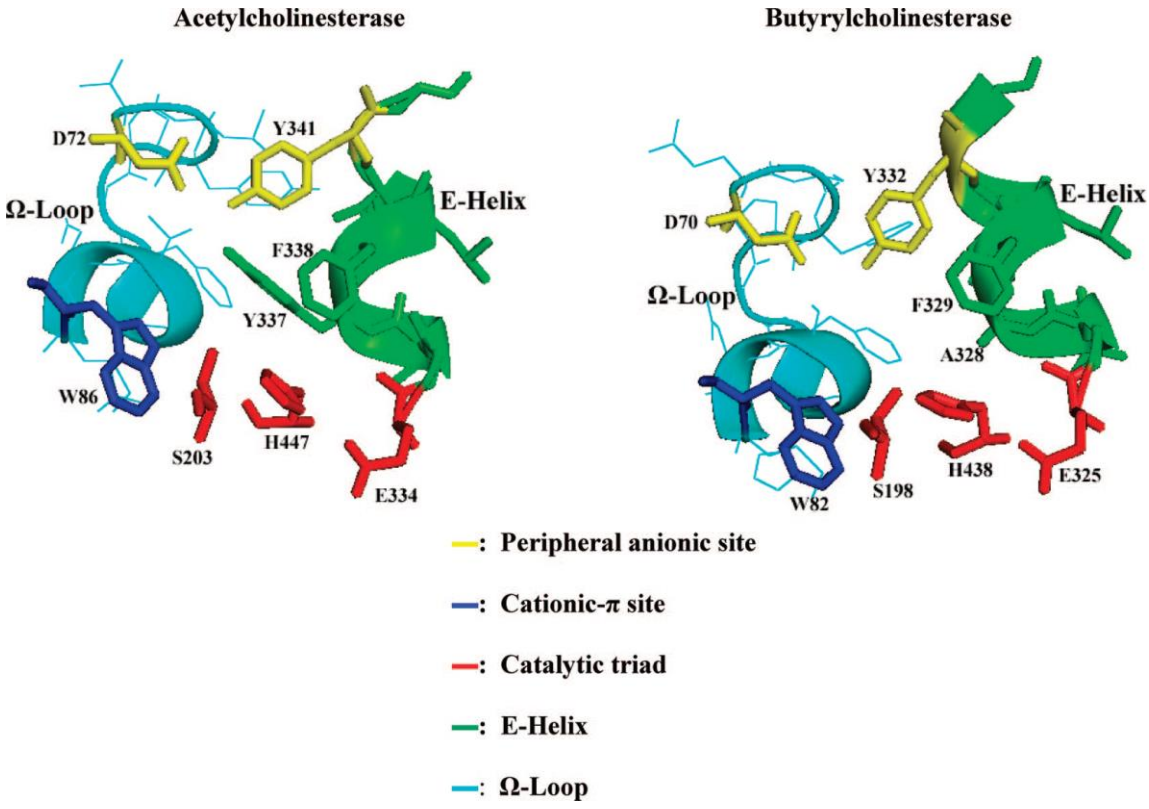

Figure 2.6. The active site of human acetylcholinestrase (huAChE; PDB: 1EVE) and human butyrylcholinesterase (huBChE; PDB: 1P0I). Adapted from Darvesh (2008).

2.4. Genetic Variants of Butyrylcholinesterase

The genetic polymorphism of BChE dictates: (i) its level of serum activity; (ii) its functional properties such as its specificity and sensitivity for substrates. Different variants exhibit different ability to hydrolyze certain xenobiotics; and conversely, are suppressed at different rates when exposed to certain chemical nerve agents (Lockridge *et al.,* 2016). Thus far, succinylcholine is the only drug which obviously induces clinical defects in persons with rare BChE genetic variant (Tunek and Svensson, 1988). Some of the common genetic variants of BChE include: atypical, K variant, fluoride, and silent (La Du *et al.,* 1990).

2.4.1. Atypical

All atypicals that have been sequenced so far have a substitution at nucleotide 209, where A replaces G and subsequently alters codon 70 from aspartic acid to glycine (McGuire *et al.*, 1989). Atypical BChE possess the kinetic features of an enzyme with deficient anionic site (La Du *et al.,* 1990). Lockridge and La Du (1978) reported that atypical BChE has a low affinity for neutral substrates but a normal turnover number, K_{cat}. Apparently, it could be safe to speculate that Asp 70 is an essential component of the anionic site.

2.4.2. K Variant

This variant is associated with 33% decrease in serum BChE activity (Rubinstein *et al.*, 1978). It is a result of linkage disequilibrium as it occurs on the same BChE chromosomal strand carrying the atypical phenotype. The mutation leading to this genetic variant was discovered at nucleotide 1615 where G was substituted with A, and the codon 539 altered from alanine to threonine. Although the most common BChE mutation, the clinical significance of this variant is only pronounced when it occurs in synchrony with atypical BChE (Bartels *et al.,* 1989).

2.4.3. Fluoride

The fluoride phenotype resists the inhibitor NaF. Two mutations that engender the fluoride phenotype have been discovered, namely: Flouride-1 and Flouride-2. Flouride-1 occurs at

the nucleotide 728 where C is substituted with G, thereby altering codon 243 from Threonine to Methionine. The other (Flouride-2) occurs at nucleotide 1169 with G replaced by T, resulting in alteration of codon 390 from Glycine to Valine (La Du *et al.*, 1990). Fluoride-1 is the first fluoride mutation discovered through DNA sequencing and the second being fluoride-2 (Nogueira *et al.*, 1992).

2.4.4. Silent

The silent phenotype is marked by little or no BChE activity, or activity far below 2% of normal (Rubinstein *et al.*, 1970). Nogueira *et al.* discovered a type of silent mutation referred to as silent-1 mutation; and it is a complicated mutation in which the T at nucleotide 351 is substituted by two nucleotides, AG. Protein synthesis is prematurely abated because a frame shift caused a stop codon to emerge at codon 129. A truncated (22% the length of typical enzyme) and inactive BChE that has lost its active serine at position 198 is therefore synthesized. The serum from this phenotype has no activity with benzoylcholine and alpha-naphthylacetate; and besides, does not react with antibody against human serum BChE (Nogueira *et al.*, 1990). The likelihood of silent-2 has been mooted; given that a different serum with the silent phenotype exhibited zero activity and absence of cross-reactive material, yet did not contain the above mutation (Aspagaus *et al.*, 1990).

2.5. Distribution of Butyrylcholinesterase in Human Tissue

The plasma, liver, skin and leg muscle respectively are considered the best source of BChE enzyme (Lockridge, 2014). Northern blot analysis (Jbilo *et al.*, 1994) has revealed that the most predominant human BChE mRNA was in the lung, liver, brain and heart. This revelation is in sync with the relative BChE enzyme content in lung, liver and brain. Curiously, the heart seemingly has more BChE mRNA than would be imagined from the little enzyme content captured below.

Table 1. Summary of Butyrylcholinesterase enzyme distribution in adult human body. Modified from Lockridge (2014).

Tissue	Weight of tissue, g	BChE, mg
Plasma	3,500	16
Liver	1,400–1,500	13
Skin	4,000–5,000	7
Leg muscle	3,500	6
Small intestine	800–900	
Lungs	400	
Cerebral cortex	1200	3
Stomach	300	1.8
Spleen	150–200	1
Kidney	130–160	1
Cerebellum	150	0.8
Heart	**300**	**0.6**
Medulla oblongata	20–25	0.085
Thyroid	20	0.0085

2.6. Functions of Butyrylcholinestrase

The existence of healthy individuals with 'silent' BChE aroused curiosity about the physiological significance of the BChE enzyme. Girard *et al.* (2007) observed that in AChE knock-out mice, BChE may act as surrogate of AChE in the central nervous system and at neuromuscular junctions. Myriad functions, both enzymatic and non-enzymatic, have been attributed to BChE.

2.6.1. Detoxification

Butyrylcholinesterase executes a very important role in the detoxification of poisons that have been ingested or inhaled. It hydrolyzes naturally occurring toxicants like physostigmine (eserine) in the calabar bean and cocaine in the leaves of the coca plant to inactive by-products. Also, BChE scavenges and destroys organophosphorus esters, including pesticides, nerve agents and a neurotoxic and anticholinesterase called anatoxin-a(s) formed by the blue-green alga *Anabaena flosaque* (Mahmood and Carmichael, 1987). More so, aspirin is hydrolyzed to sialic acid by BChE (Lockridge, 2014). The action of BChE converts heroin (a diester) to morphine (Lockridge, 2014). BChE again converts a precursor drug, bambuterol to active antiasthma drug, Terbutaline (Barricklow and Blatnik, 2013).

2.6.2. Acetylcholine Hydrolysis

Lockridge *et al.* indicated that BChE hydrolyzes the neurotransmitter acetylcholine in their studies with AChE and BChE knock-out mice (Lockridge *et al.*, 2011). Before this, Boudinot *et al.* (2005) and Duysen *et al.* (2007) had stated that huperzine A and donepezil, both Alzheimer drugs, inhibit AChE but not BChE. Indeed, the toxic effects of these drugs have not been observed in AChE knock-out mice with normal levels of BChE. Duysen *et al.* (2007) further added that BChE deficient mice with normal levels of AChE die from a symptom of excess acetylcholine called tonic convulsion after been treated subcutaneously with 1.5 mg kg^{-1} huperzine and 10 mg kg^{-1} donepezil. From the foregoing, it could therefore be rationalized that BChE acts in crises situation to dispose of the physiological role of AChE (that is hydrolysis of acetylcholine).

2.6.3. Fat Metabolism

BChE hydrolyzes ghrelin even beyond nanomolar peptide concentrations to desacyl ghrelin and octanoic acid (De vriese *et al.*, 2004). Octanoyl ghrelin is a 28 amino acid containing peptide that has been esterified on Ser3 to octanoic acid (De vriese *et al.*, 2004). BChE knock-out mice turn obese when placed on a high fat diet, not the wild-type though. BChE deficiency is believed to contribute to decreased fat breakdown (Lockridge, 2015).

2.6.4. Scavenger of Polyproline-Rich Peptides

Biberoglu *et al.* (2013) reported that a mass spectrometric study of plasma BChE suggests a putative function for BChE in scavenging peptides rich in polyproline. The authors further stated that the four homologous subunits that constitute the BChE tetramer are wound around one polyproline-rich peptide. Polyprotein-rich regions in proteins partake in protein-protein interaction with effects on cell motility, signaling, transcription, elasticity, immune respond and self-assembly (Adzhubei *et al.,* 2013). By sequestering polyproline-rich peptides into the structure of BChE, they are cut off from interacting with potential proteins, thus protecting cells from unregulated signaling.

2.7. Neurodegeneration

Neurodegeneration has been defined as the progressive attenuation/loss of structure and function or even death of neuronal cells (Mann, 1996). Dementia is a consequence of neurodegeneration, and its most common form is the Alzheimer disease.

AD progressively and significantly ruins brain structure and function. It is characterized by the continuous depletion of cortical neurons that mediate advanced cognitive activities (Norfray and Provenzale, 2004). AD disrupts synaptic function early in the disease process, impeding communication in the neural circuits remarkable for memory and yet other cognitive activities. AD linked degeneration starts within the medial temporal lobe, mainly in the hippo campus and entorhinal cortex (Jack *et al.*, 1997). Injury to these brain structures leads to learning deficit and memory loss. The deterioration then spreads over the temporal association cortex, then to parietal areas (Holtzman *et al.*, 2011).

Norfray and Provenzale hypothesized that the neuronal destruction observed in AD is associated with the settling and build-up of abnormal proteins within and beyond the neurons. And this represents the hallmark of plaques and tangles. The abnormal proteins settle in the cerebral cortex due to the archetypal manner of expansion along neural pathways responsible for mediation of memory and myriad cognitive functions (Norfray and Provenzale, 2004). Senile plaques are extracellular build-up of amyloid proteins and are made up of insoluble amyloid-beta protein (Aβ). Querfurth submitted that cells throughout life usually liberate soluble Aβ after breakdown of the amyloid precursor protein (APP). AD results from abnormal cleavage of APP that engenders the settling of Aβ into dense beta sheets and leads to the development of senile plaques (Querfurth, 2010).

2.7.1. The Cholinergic Hypothesis and Role of Butyrylcholinesterase in Alzheimer's

Cholinergic neurotransmission in the central nervous system (CNS) of mammals is controlled largely by AChE which catalyzes the hydrolytic cleavage of acetylcholine, the cholinergic neurotransmitter (Silver, 1974). The indication that there is a substantial loss of cholinergic neurons in the brain of AD patients coupled with the decreased activity of choline acetyltransferase (ChAT); and ultimately, diminished neurotransmission and cognitive dysfunctions lead to the cholinergic hypothesis (Gauthier, 2002). Besides, a decrease in nicotinic and muscarinic receptors has been reported (Francis *et al.*, 2010). Liston *et al.* (2004) observed that by utilizing cholinesterase inhibitors, the amount of acetylcholine which has a vital role in cognitive functions can be restored. Presently, research has been directed on the quest for BChE inhibitors (Carolan *et al.*, 2010; Nawaz *et al.*, 2011). In AChE knock-out mice especially, BChE ensure the perpetual control of cholinergic neurotransmission by compensating for the deficiency of AChE. This reinforces the significance of BChE in cholinergic neurotransmission (Li *et al.*, 2000). According to Giacobini (2004), BChE is seemingly unaffected by changes taking place in the AD brain while the activity of AChE obviously plummets. Therefore, in AD brain where there is little or no acetylcholine, BChE assumes a pivotal role in cholinergic transmission thus promoting further cognitive decline. Lane *et al.* (2006) reported that the amount of free acetylcholine available to interact with neuronal receptor is enhanced with

the inhibition of both AChE and BChE. In an experiment using adult rats, Greig *et al.* (2005) demonstrated that selective inhibition of BChE augmented acetylcholine level, decreased amyloid deposit and raised cognitive function. And essentially, Podoly *et al.* (2009) advanced that researchers have discovered a connection between the K variant of BChE and low vulnerability to develop AD.

2.7.2. The Amyloid Hypothesis

This hypothesis holds that rise in the beta amyloid (Aβ) protein in the brain induces a sequence of events that results in Alzheimer disease, and that targeting Aβ could bring about a reduction, or even terminate, the stream of AD progression (Giordano *et al*., 2005). Amyloid plaques comprises amyloid beta (Aβ) peptides that aggregate to form extracellular clusters hindering neuronal function and triggering neurotoxicity (Lorenzo and Yankner, 1994). Turner *et al.* contends that the proteolytic breakdown of amyloid precursor protein (APP) engenders Aβ1-40/42 peptides which have been identified as the neurotoxic species of Aβ. As an integral membrane protein, APP is ubiquitous in the biological system and is presumed to control myriad processes such as neural plasticity and synapse formation (Turner *et al*., 2003) in addition to dendritic spine formation as well as maintenance (Lee *et al*., 2010). There are two ways of processing APP. One is via the amyloidogenic pathway which generates Aβ as a result of its cleavage by β- and γ-secretase; and the second is through the non-amyloidogenic pathway where α- and γ-secretase cleaves APP which leads to the production of the non-toxic component called α-sAPP. It has been demonstrated that a link exist between BChE and the evolution of Aβ fibrils (Lockridge, 2011) and that the excitement of muscarinic acetylcholine receptors enhances the non-amyloidogenic pathway and ultimately connects the cholinergic and amyloid hypothesis (Giordano *et al*., 2005)

2.8. Amitriptyline

Tricyclic antidepressants (TCAs) are predominantly used in the therapy of major depression disorders. Amitriptyline (AMI) is a clinical TCA extensively used for the treatment of chronic pain, depressive disorders and prophylactic therapy of migraine (Schmider *et al.*, 1995). Chemically, AMI is 3-(10, 11- dihydro-5H-dibenzo [a,d]

cycloheptane-5-ylidene)-N,N-dimethyl-1-propanamine hydrochloride with $C_{20}H_{23}N$,HCL as its molecular formula and 313.9 as its formula weight. AMI essentially exudes its action as a serotonin-norepinephrine re-uptake inhibitor. Aaltonen *et al.* (1985) and Cokugras (2003) stated that some of its anticholinergic side effects manifest in symptoms such as dry mouth, cardiovascular dysfunction, constipation, delirium, sinus tachycardia, memory impairment, and blurred vision. It has been reported that these side effects are triggered by the inhibition of cholinesterase (Perkinson *et al.*, 1969) or are end result of the antagonizing reactions of TCAs on the cholinergic receptors in the brain (Schein and Smith, 1978) or both. Documented evidence abounds on the inhibitory potency of AMI against AChE from erythrocyte membrane (Muller, 2002) and from cerebral cortex (Barcellos, 1998).

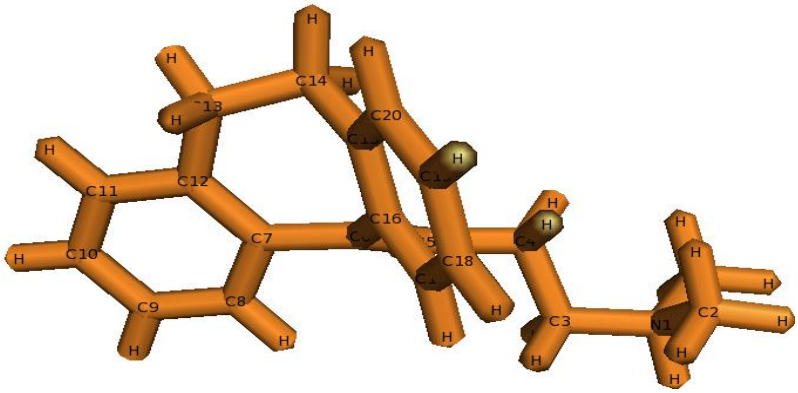

Figure 2.7. Chemical structure of amitriptyline. 3D structure generated using Corina (accessed via: https://www.mn-am.com/online_demos/corina_demo) and visualized with PyMOL (The PyMOL Molecular Graphics System, Schrödinger LCC, open source v.1.2x. http://www.pymol.org).

2.8.1. Pharmacokinetics of Amitriptyline

Amitriptyline is an exceedingly lipophilic drug that goes through extensive metabolism. After it is administered orally, its bioavailability is 47±11%. This is a result of first pass effect (Schulz *et al.*, 1983). AMI is a putative substrate for P-glycoprotein (ABCBAI) transporter at hepato-biliary and intestinal level (Abaut, 2007; Abaut, 2009). Hence, this might possibly account for its low bioavailability. Upon intravenous administration, AMI terminal half-life varies between 15 to 19h (Jorgensen and Hansen, 1976); and when

administered orally, it ranges from 17 to 26h (Burch and Hullin, 1981). It undergoes extensive metabolism basically by N-demethylation, producing nortriptyline (NOR) its active metabolite, and to a lesser degree by N-oxidation and hydroxylation (Kruger *et al.*, 1986). There is a huge individual variation in the formation of nortriptyline from amitriptyline (Rollins *et al.,* 1980). Different cytochromes partake in amitriptyline metabolism. AMI and NOR hydrolysis is catalyzed by CYP2D6 whereas the demethylation of AMI and NOR is mediated by CYP2C19 and CYP3A4. There is also the likelihood of the clinical significance of AMI metabolic pathway given that genetic polymorphism may highlight the higher or lower susceptibilities of adverse reactions (Steimer *et al.,* 2005) and possibly life threatening drug-drug reaction (Newberry *et al.,* 1997; Castberg *et al.,* 2005).

2.8.2. Pharmacodynamics of Amitriptyline

AMI has multiple and varied pharmacological targets and this perhaps explains why it is a rather unselective drug when placed in comparison with new antidepressants. Though this nonselectivity is responsible for its toxicity, it could also possibly account for its effectiveness in chronic pain treatment. There is no gainsaying that the antidepressant and antinociceptive action of AMI and NOR are essentially but not solely due to its ability to bind serotonin and noradrenaline transporters at central sites (Mico *et al.,* 2006; Verdu *et al.,* 2008). It has been hypothesized that the antinociceptive efficiency of AMI is regulated by other peripheral and central mechanisms of action namely: α_2 adrenergic receptor agonism, $GABA_B$ receptor potentiation, 5-HT_2 receptor antagonism, blockade of Na^+ and K^+ channel activation and ca^{2+} channels action, activation of the endogenous opioid system, decrease in prostaglandin E_2 and TNFα production, and glutamate NMDA receptor antagonism (Mico *et al.,* 2006; Verdu *et al.,* 2008).

2.9. Molecular Docking

Interactions between proteins and their ligands are fundamental to life. Living organisms by virtue of these interactions maintain a system of regulatory and metabolic communication networks that make up the processes of life. Comprehending the nexus of metabolic pathways and the communication between a protein and its ligand has become

necessary and molecular docking has served this need. Molecular docking may be defined as a concept of structural bioinformatics which serve solutions to unravel the mechanism behind protein-ligand interactions and some other kind of biomolecular interactions. It enables the interacting molecule to bind together by way of their topography. The goal of docking is to find out the best viable conformation of protein–ligand; or possibly, other kind of interactions using minimal energy (Mukesh and Rakesh, 2011; Guedes, 2014). This docking approach is an effective way to model the interaction between protein and small molecule at the molecular level. It helps in profiling the behavior of these molecules at their sites of binding (Ferreira *et al.,* 2015). The two main approaches used in docking involves firstly acquiring a stable ligand conformation and secondly evaluating its binding strength, and in many cases, binding sites are estimated before carrying out docking. Generally, binding sites are identified through comparison of the target of interest with other proteins sharing similar function and from same family (Gschwend *et al.,* 1996). The molecular docking mechanism, which started with the "lock and key" model, has since evolved a great deal. "Induced-fit" model was considered as a logical transformation of the primitive lock and key model, where a conformational change is induced in the active site depending on the binding ligand (Lamb and Jorgensen, 1997). The applications of molecular docking are widespread whilst the information gleaned is profound. And also, it has open a new vista into the arena of research which focuses on target discovery, lead molecule designing, and analyzing application possibility of compounds (Shoichet *et al.*, 2002).

3. MATERIALS AND METHODS

3.1. Enzyme and Chemicals

Butyrylcholinesterase (BChE) from equine serum, S-butyrylthiocholine (BTCh) iodide, 5,5[1] dithiobis[2-nitrobenzoic acid] (DTNB), Methanol, Potassium hydroxide, 3-(N-morpholino) propane sulfonic acid (MOPS) and amitriptyline hydrochloride were obtained from sigma Aldrich (St. Louis, MO, USA). All other reagents utilized were of analytical grade.

3.2. Protein Concentration Determination

A NanoDrop spectrophotometer was used to quantify the protein. The concentration of protein was calculated using Warburg–Christian and Kalb–Bernlohr Methods.

3.3. Reagents Preparation

3.3.1. 200 mM MOPS/KOH, pH 7.5, volume 250 mL

a. 10.46 g of MOPS was weighed using electronic weighing balance. This was dissolved in 200 mL of distilled water. A clear solution was attained with the aid of the magnetic stirrer.

b. 28 g of KOH was also weighed using electronic weighing balance. This was also dissolved in 50 mL of distilled water. A clear solution was eventually made with the aid of the magnetic stirrer. The concentration of the KOH solution was 10 M.

c. The pH of the MOPS buffer was adjusted to 7.5 by adding 10 M KOH in drops while simultaneous stirred using magnetic stirrer. The final volume was then made up to 250 mL with distilled water. Thus, 200 mM MOPS/KOH buffer at pH 7.5 was obtained.

3.3.2. 20 mM MOPS/KOH, pH 7.5, volume 200 mL

200 mM MOPS/KOH, pH 7.5 buffer was diluted 10 times using distilled water. Thus, 20 mM MOPS/KOH at pH 7.5 buffer was prepared.

3.3.3. Substrate (Butyrylthiocholine) and 5,5^{I} – Dithio-Bis (2-Nitro Benzoic acid)

a. 19.03 mg butyrylthiocholine iodide was weighed and dissolved in 1200 µL of 20 mM MOPS/KOH of pH 7.5. This made the stock BTCh concentration 50 mM.

b. 5.94 mg 5,5[1] dithio-bis (2-nitro benzoic acid) was weighed and dissolve in 6 mL of 200 mM MOPS/KOH of pH 7.5 to attain a stock DTNB concentration of 2.5 mM

3.3.4. Inhibitor (Amitriptyline)

15.7 mg of AMI was dissolved in 1,000 µl of methanol to make 50 mM stock solution; and was serially diluted to 25 mM, 12.5 mM, 6.25 mM, 3.125 mM, 1.56 mM, 0.7815 mM, 0.391 mM, 0.195 mM, 0.0977 mM, 0.0488 mM and 0.0244 mM respectively. These were the working solutions used to screen for the inhibitory activity of AMI against BChE. Given that only 5 µl of the foregoing stock was added to the reaction mixture to make a total volume of 500 µl (1:100 dilution) during the assay, the final concentrations in the reaction mixture corresponded to 250 µM, 125 µM, 62.5 µM, 31.25 µM, 15.625 µM, 7.8125 µM, 3.906 µM, 1.953 µM, 0.977 µM, 0.488 µM and 0.244 µM respectively.

3.3.5. Enzyme Dilution

BChE was diluted 1:1000 with 20 mM MOPS/KOH, pH 7.5 buffer.

3.4. Butyrylcholinesterase Activity Assay

Kinetic studies were performed to find out Michaelis-Menten constants (K_m and V_m). Using Perkin Elmer Lambda 25 UV/VIS, enzyme activity was measured spectrophotometrically according to the method of Ellman *et al.* (1961). BChE activity was measured at 37^0C under the following conditions: 250 µl of 200 mM MOPS/KOH buffer (pH 7.5), 165 µl of distilled water, 10 µl of BTCh iodide at increasing concentrations from 0.05 mM, 0.1 mM, 0.25 mM, 0.50 mM, 1 mM to 2 mM, 50 µl of 2.5 mM DTNB and 25 µl of BChE in the absence of amitriptyline. The concentration of BChE in the assay medium was 5 µg ml^{-1}. The reaction was started in each case with the addition of BChE. Assay was conducted in triplicates and the readings were taken after 20 s in each case. The reaction was observed to be linear within this period. During the experiment, a

blank tube which contains all compounds and additional 25 µl of 20 mM MOPS/KOH, pH 7.5 buffer (instead of BChE) was made use of in other to eliminate the spontaneous hydrolysis of butyrylthiocholine.

Specific activity was calculated from the average activity readings and with this Michaelis-Menten, Lineweaver-Burk, Dixon and other plots were generated (Segel, 1975). Specific Activity (Units/mg Protein) = $\frac{\Delta Abs412 * Vt}{13.6 * Vs * [Protein]}$

Δ Abs 412 / min: Absorbance change per minute at 412 nm

Vt: Total volume of assay medium (500 µl)

Vs: Sample volume (25 µl)

13.6: Extinction coefficient of 5-thio-2-nitrobenzoic acid (mM)

[Protein]: concentration of protein in mg ml^{-1}

3.5. Butyrylcholinesterase Inhibition Assay

The ability of AMI to inhibit BChE purified from equine serum was tested. AMI was prepared as explained in section 3.3.4. The activity of BChE without either AMI or methanol was measured in accordance with Ellman *et al.* (1961) procedure at 412 nm for 20 s. As a reference, the activity of BChE in the reaction mixture containing 5 µl of methanol instead of the inhibitor was measured. This served as a baseline (control) for subsequent measurements in the presence of AMI (test sample). The concentration of methanol in the assay mixture was 1%. Methanol at this concentration exhibited infinitesimal inhibitory effect on BChE. The reaction medium contained 250 µl of 200 mM MOPS/KOH pH 7.5, 160 µl of dH_2O, 10 µl of 50 mM BTCh, 50 µl of 2.5 mM DTNB, 5 µl of AMI prepared at varied concentrations and 25 µl of BChE. The final concentrations of AMI in the assay medium were: 0.244 µM, 0.488 µM, 0.977 µM, 1.953 µM, 3.906 µM, 7.8125 µM, 15.625 µM, 31.25 µM, 62.5 µM and 125 µM. The reaction was initiated with the addition of BChE after rapid and immediate mixing and the absorbance was measured at 412 nm for 20 s. BChE had the concentration of 5 µg ml^{-1} in the reaction mixture. Assay was performed in triplicates. A blank tube consisting of all compounds except BChE was utilized during the assay. The half maximal inhibitory concentration (IC_{50}) of AMI against

BChE was estimated from the eventual plot of percentage remaining activity against inhibitor concentration. Percent remaining activity was computed as below:

$$\text{Percent remaining activity (\%)} = \frac{Abs\ control - (Abs\ control - Abs\ test\ sample)}{Absorbance\ of\ control} \text{x}100$$

3.6. Kinetic Studies of Butyrylcholinesterase Inhibition

The essence of performing the inhibitory kinetic experiment was to find out the K_m, V_m and K_i of BChE under the influence of varying AMI and BTCh concentrations. Six different concentrations of AMI (0.25 µM, 0.5 µM, 1 µM, 2 µM, 4 µM, 8 µM) and six different BTCh concentrations (0.05 mM, 0.1 mM, 0.25 mM, 0.5 mM, 1 mM, 2 mM) were made use of in this experiment. For any fixed AMI concentration, the activity of BChE at different substrate concentrations was determined in triplicates at each stage. The assay mixture was made up of 250 µL of 200 mM MOPS/KOH, pH 7.5, 160 µL of dH_2O, 10 µL of BTCh, 50 µL of 2.5 mM DTNB, 5 µL of AMI and 25 µL of BChE. The concentration of BChE in the reaction mixture was determined as 5 µg ml^{-1}. The reaction was at each time started after the addition of enzyme and with rapid and immediate mixing. Increased in absorbance was monitored at 412 nm according to Ellman *et al.* (196l) method for 20 s. A blank tube consisting of all compounds except BChE was made use of during the assay. It is pertinent to state here that AMI and BTCh were prepared as stock solutions with different concentrations and their final concentrations stated above were only obtained after their addition to the reaction medium. Besides, the concentrations of the inhibitor were varied between stages, whilst that of the substrate were varied within stages.

3.7. Statistical Analysis

For the computation of the kinetic parameters and the determination of the inhibition type, STATISTICA ’99 Edition (Tulsa, OK, USA) was used.

3.8.1. Homology Modeling

The 3D structure of eqBChE was built by aligning a target eqBChE sequence with a template huBChE sequence. Foremost, the eqBChE (accession number P81908) was retrieved from www.uniprot.org and its protein sequence downloaded in the FASTA

format. Sequence alignment was run using CPH model (Nielsen *et al.,* 2010) and the percentage identity between the target and template sequences was observed to be about 90.4%. This indicates that it was in the safe zone (> 30%) and accuracy of the model can be compared to crystallography. Model was built based on the target-template alignment. Coordinates which were conserved between the target and the template were copied from the template to the model. Finally, the geometry of the resulting model was regularized by using a force field and the accuracy of the modeled protein evaluated using VERIFY3D (Luthy *et. al*., 1992) web server.

3.9. Molecular Docking

Molecular Docking was conducted using SwissDock. A web service that is based on the docking software EADock DSS (Grosdidier *et al.,* 2011a). SwissDock was chosen because it had a user friendly interface with a facility for input of protein and ligand structures straight from databases, alter docking parameters, and ultimately visualize the best favorable clusters on the web. More so, results obtained can be downloaded and visualized in UCSF Chimera. The region of interest x, y, and z for the putative binding site was left empty for server to predict. Docking type was fixed as exact and rigid. Binding modes having the best favorable energies were automatically estimated by Fast Analytical Continuum Treatment of Solvation (FACTS) and clustered. Binding modes were scored based on their FullFitness score and estimated ΔG. Then clusters were classified based on the average FullFitness of their elements (Grosdidier *et al*., 2007). Results produced from the SwissDock were viewed using PyMOL (The PyMOL Molecular Graphics System, Schrödinger LCC, open source v.1.2x. http://www.pymol.org).

3.10. Protein–Ligand Interaction Profiling

The total profiling of the noncovalent interactions between the eqBChE and the docked AMI was actualized by protein ligand interaction profiler, a Web server based on a python command-line application for identifying and visualizing interatomic associations in three-dimensional (3D) protein structures (Salentin *et al.,* 2015).

4. RESULTS

The *in vitro* inhibitory activity of AMI against equine serum BChE was investigated according to colorimetric procedure of Ellman *et al*. using substrate analog BTCh (Ellman *et al*., 1961). The investigation was carried out at ten varying concentrations of AMI (0.244 μM–125 μM). BTCh concentration was fixed constant at 1 mM through the entire course of the BChE inhibition experiment. BChE activity measurements were replicated three times at any given AMI concentration, and the mean specific activities were computed accordingly. AMI was discovered to cause a decrease in BChE activity in a concentration dependent fashion. Within the concentration limits investigated, the ensuing inhibition curve approached the zero point. The IC_{50} value was subsequently determined graphically to be 10 μM from the % residual activity against [AMI] curve (Fig. 4.3). With the same data, Hill plot (log(Vi/(Vo-Vi)) vs. log[AMI]) was generated and it gave an IC_{50} value of 11.75 μM (Fig. 4.4).

In the next step, substrate kinetics was carried out. The specific activity of BChE at six different BTCh concentration (0.05 mM, 0.1 mM, 0.25mM, 0.5 mM, 1 mM and 2 mM) were measured. All activity measurements were repeated three times and the average specific activities computed accordingly. In the range studied, the Michaelis-Menten plot produced a parabola (Fig. 4.1) whilst the Lineweaver-Burk plot gave a straight line cutting through the positive axis of the ordinate and the negative axis of the abscissa (Fig. 4.2).

The plot of specific activity against different enzyme concentrations at fixed AMI concentration revealed the mode of inhibition to be reversible; and based on the inhibitory activity experiments, six different AMI concentrations (0.25 μM, 0.5 μM, 1 μM, 2 μM, 4 μM and 8 μM) were selected from the region where the inhibition was found to be linear. These concentrations were subsequently tested in the inhibitory kinetic studies at varying BTCh concentrations (0.05 mM, 0.1 mM, 0.25mM, 0.5 mM, 1 mM and 2 mM). All activity readings were taken in triplicates, and the computed specific activities were used to generate the Michaelis–Menten plot (Fig.4.6), Lineweaver–Burk plot (Fig. 4.7) and Dixon plot (Fig. 4.9). From the data extracted from the Lineweaver–Burk and Dixon plots, their secondary replots (Fig. 4.8 and Fig. 4.10; 4.11) were made respectively. These plots

were used to graphically determine both the inhibition type and the kinetic parameters. The nature of inhibition was linear-mixed type (Fig. 4.7) with a preponderance of partial competitive component (Fig 4.10). The kinetic constants: α, K_s, K_i, αK_i and V_m are presented in Table 2.

In the subsequent step, *in silico* studies were performed to predict the plausible inhibitor–binding pocket of eqBChE. AMI was docked against eqBChE (Fig. 4.12) modeled from huBChE 3O9M. In order to reduce bias, a blind docking approach was employed. In this way, the translational search area involved the entire enzyme surface. The top docking solution explicitly showed that AMI was localized at the bottom of the BChE active site gorge (Fig. 4.14). The highest-ranked docking pose of AMI ($\triangle G$ = -2.92) seemingly forged hydrophobic bonds with Leu286, Val288, Trp231, Phe329 and Tyr332. The aromatic rings of AMI also formed л–π stacking with Phe329 and Trp231 of eqBChE. Again, the tertiary amine nitrogen of AMI established an electrostatic interactions with Glu197 adjacent to Ser198 of the catalytic triad (Fig. 4.15). To account for the slight noncompetitive nature of the mixed type inhibition, AMI was further re-docked against the modeled eqBChE that already had BTCh docked, and their interactions were studied (Fig. 4.17A & B). In this case, AMI was found to have interacted exclusively with PAS residues, establishing an electrostatic interaction (salt bridge) with Asp70 and even yet hydrophobic interactions with both Asp70 and Tyr332 (Fig. 4.18).

4.1. Substrate Kinetics

Kinetic parameters for the BChE were determined by using different concentrations of BTCh while maintaing the DTNB concentration constant (0.25 mM). In the reaction mixture, final concentrations of BTCh were 0.05 mM, 0.1 mM, 0.25 mM, 0.50 mM, 1 mM and 2 mM. For each concentration, activity measurements were repeated three times and the average specific activities were computed accordingly. In the range studied, the plot produced a parabola (Fig. 4.1) indicating that the hydrolytic cleavage of BTCh by BChE obeyed Michaelis Menten Kinetics. The double reciprocal plot (Fig 4.2) was equally drawn from the same data, and the kinetic constants were determined from the points of intersection on the ordinate and abscissa.

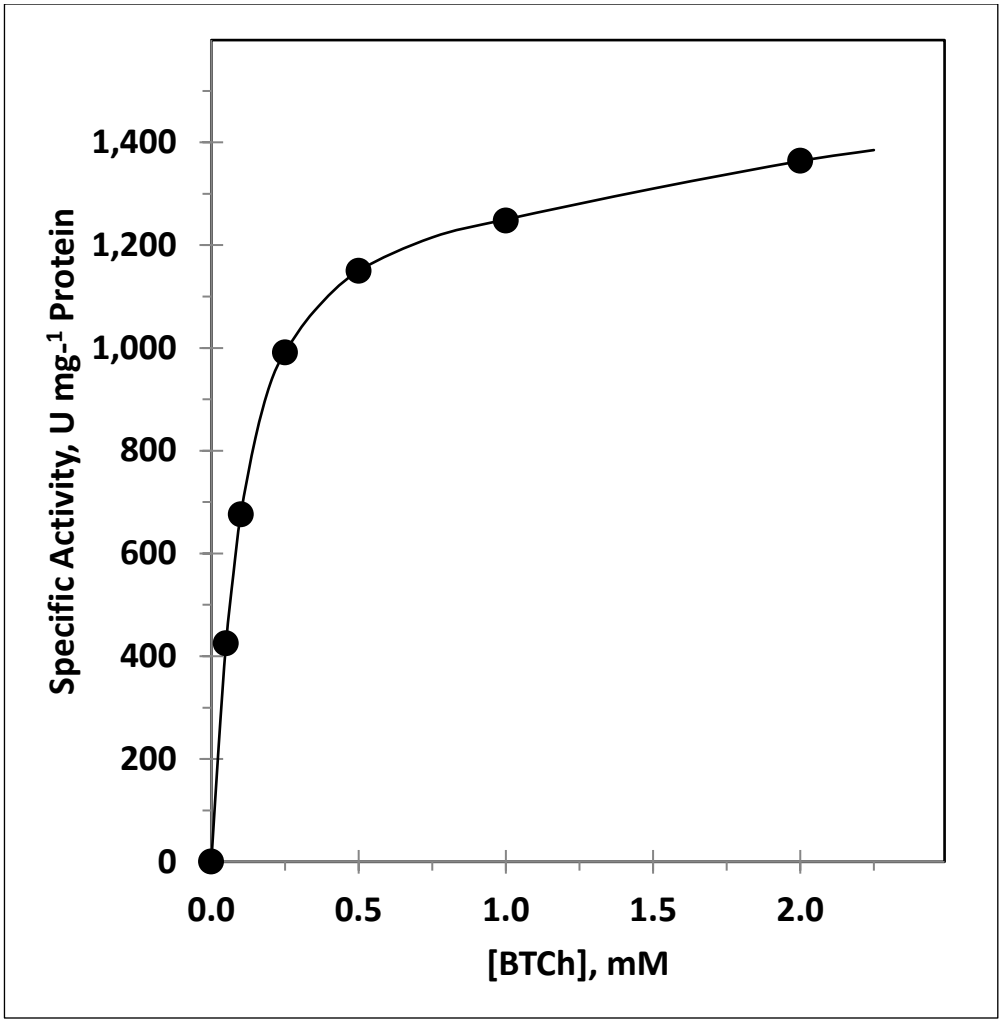

Figure 4.1. Michaelis Menten plot of the behavior of BChE at varying concentrations (0.05 mM–2 mM) of the substrate BTCh. Each data point is the average of three measurements.

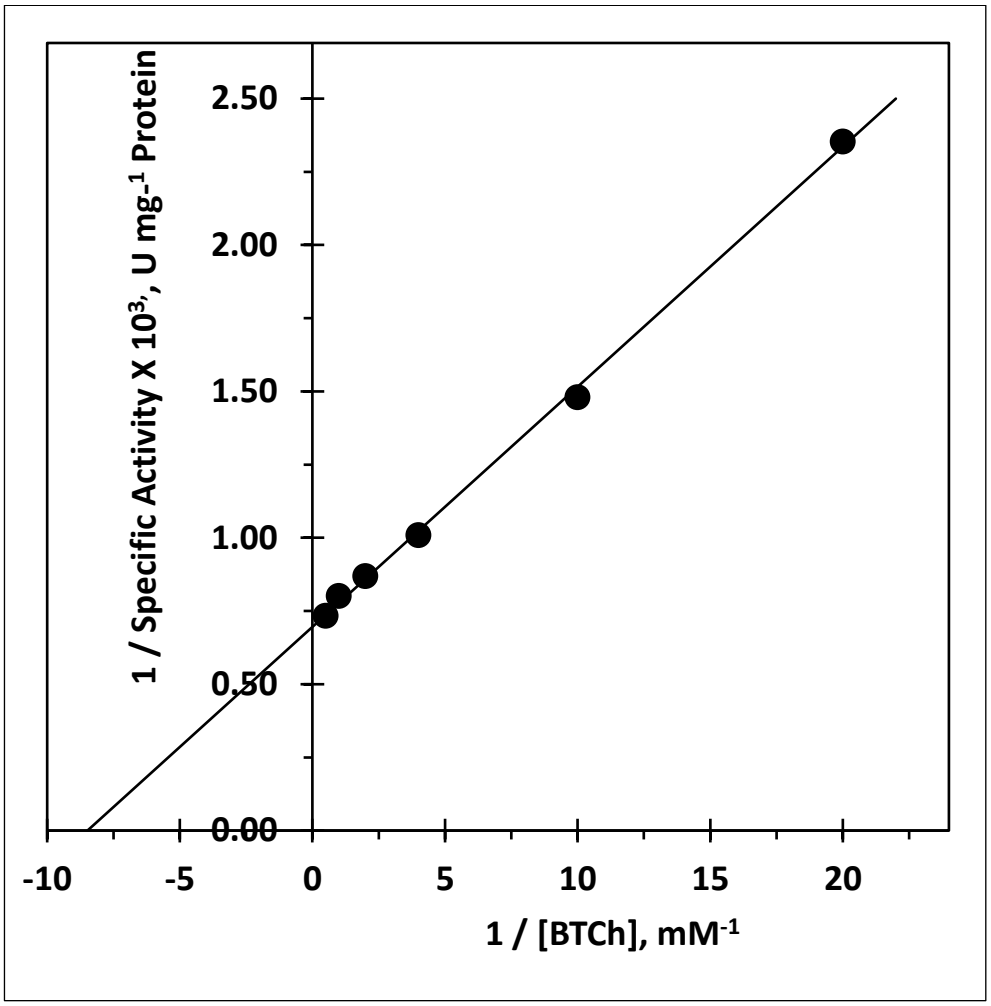

Figure 4.2. Double reciprocal plot of the steady-state kinetic behavior of BChE at different substrate (BTCh) concentrations (0.05 mM–2 mM). Each data point is the average of three measurements.

4.2. Effect of Amitriptyline Concentration on Butyrylcholinesterase Activity

Using substrate analog (BTCh), the inhibitory activity of AMI against equine serum BChE was investigated according to colorimetric procedure of Ellman *et al*. (Ellman *et al*., 1961). The tricyclic antidepressant was found to alter the activity of BChE purified from equine serum. This experiment was carried out at ten varying concentrations of AMI (0.244 μM–125 μM). BTCh concentration was fixed constant at 1 mM through the entire course of the BChE inhibition experiment. BChE activity measurements were replicated three times at any given AMI concentration, and the mean specific activities were computed accordingly. AMI was found to cause a reduction in BChE activity in a concentration dependent fashion. Within the concentration limits studied, the resulting inhibition curve did not reach the zero point, even though a gradual decrease in BChE activity was noticed. The IC_{50} value was subsequently determined graphically to be 10 μM from the % remaining activity against [AMI] plot (Fig. 4.3). With the same data, Hill plot ($\log(Vi/(Vo-Vi))$ vs. log[AMI]) was generated and it gave an IC_{50} value of 11.75 μM (Fig. 4.4).

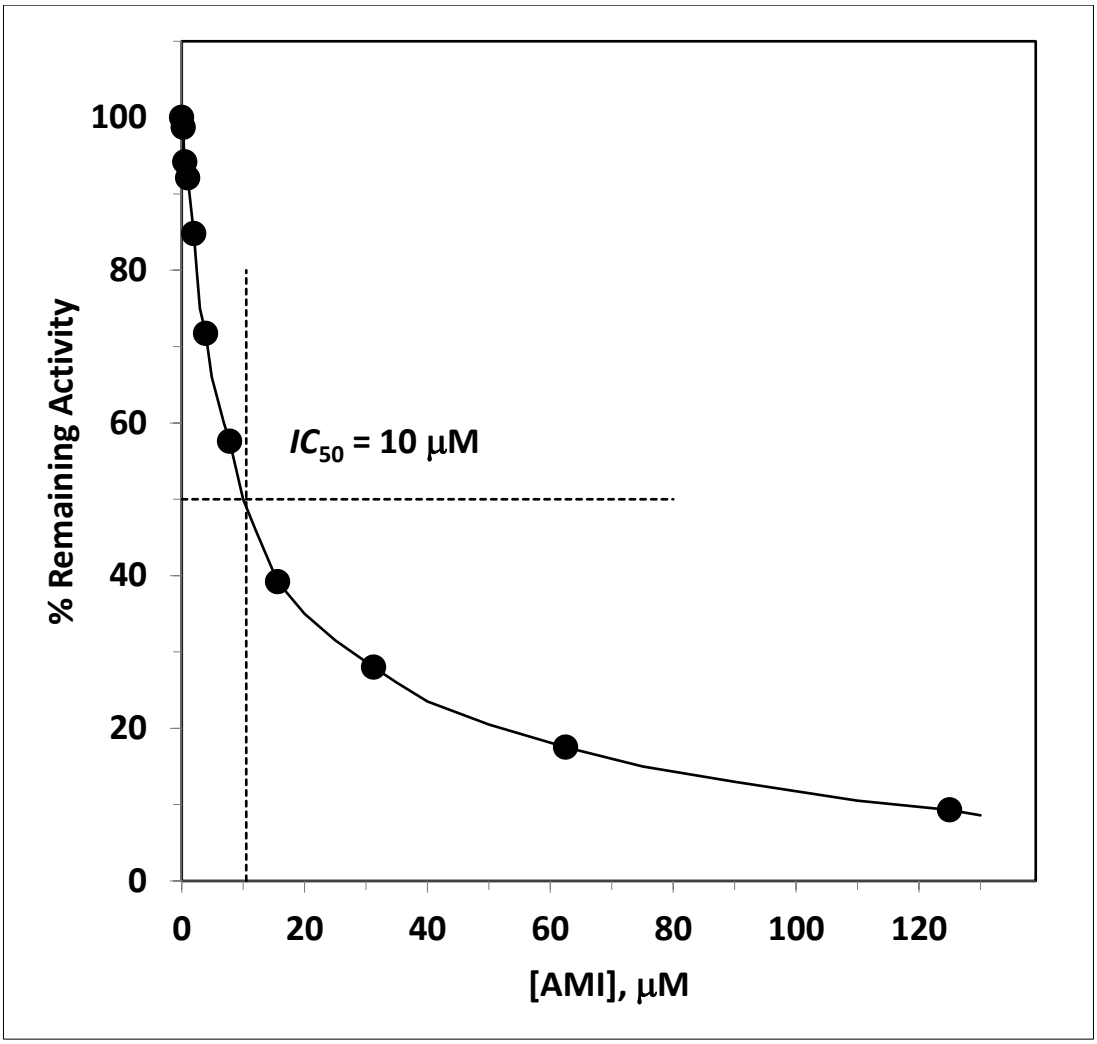

Figure 4.3. Dose-dependent inhibition of purified equine BChE activity by different concentrations of AMI (0.244 μM–125 μM) in the presence of 1 mM BTCh. Each data point is a mean of three measurements.

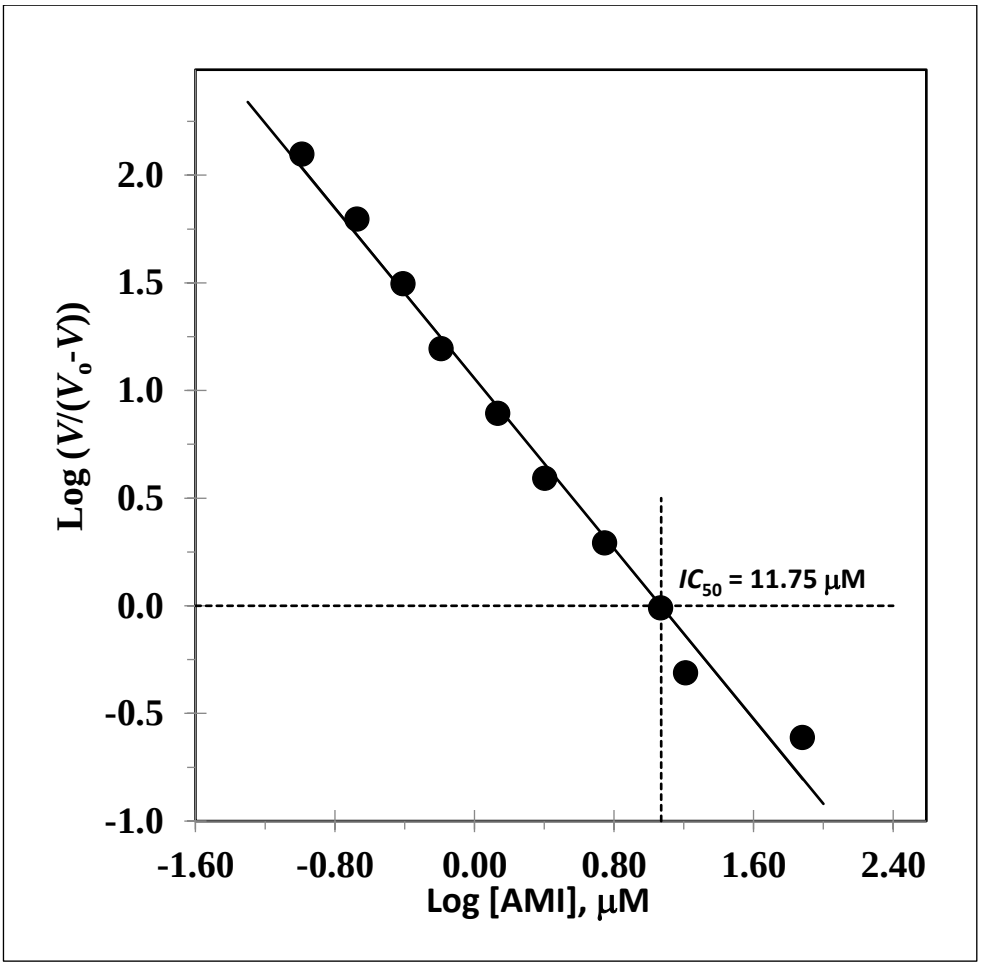

Figure 4.4. The Hill plot (*i.e.*, log ($V/(V_0 - V)$) versus log [AMI]) of BChE inhibition by AMI. Each data point is an average of three determinations.

4.3. Determination of the Reversibility or Otherwise of Amitriptyline Induced Inhibition of Butyrylcholinesterase

Before conducting the kinetic studies on butyrylcholinesterase inhibition, a preliminary experiment was carried out to determine whether the mode of inhibition by AMI was reversible or irreversible. The activity of the enzyme was determine at different enzyme concentrations. Different volumes of the stock enzyme ranging from 2.5 µl, 5 µl, 7.5 µl, 15 µl, 20 µl, 25 µl to 30 µl were periodically added to the reaction mixture that contained a fixed 10 µM AMI concentration and the activities of the enzyme was measured spectrophotometrically according to Ellman *et al*. (1961) method. All activity measurements were done in triplicates and from the data obtained, specific activity was calculated. The plot of specific activity versus enzyme concentration was subsequently generated, and from the resulting plot, a reversible mode of inhibition was confirmed.

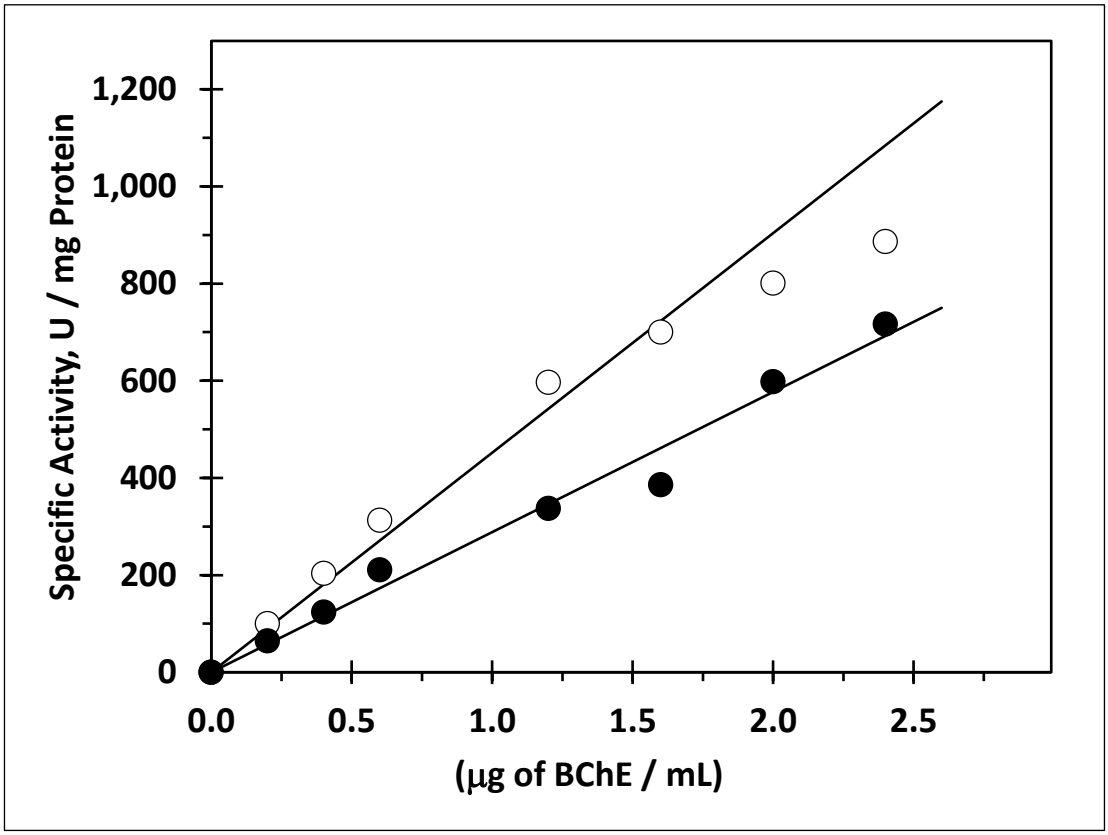

Fig 4.5. Plot of specific activity versus different enzyme concentrations. Each data point is the average of three different absorbance readings.

4.4 Effect of Amitriptyline on the Steady-State Kinetic Behavior of Butyrylcholinesterase

The confirmation of reversible mode of inhibition by AMI set the stage for the conduct of kinetic studies in order to understand its inhibition mechanism. Six different concentrations of AMI (0.25 μM, 0.5 μM, 1 μM, 2 μM, 4 μM and 8 μM) were chosen from the region where the inhibition was discovered to be linear in the inhibitory activity experiment (section 4.2). These concentrations were subsequently utilized in the inhibitory kinetic studies at varying BTCh concentrations (0.05 mM, 0.1 mM, 0.25mM, 0.5 mM, 1 mM and 2 mM). All activity readings were taken in triplicates and the mean specific activity calculated accordingly. The Michaelis–Menten plot (Fig. 4.6) in the absence and in the presence of varying concentrations of AMI was plotted. From the same data, Lineweaver–Burk plot (Fig. 4.7) in the absence and in the presence of varying concentrations of AMI was equally generated. The nature of inhibition was deciphered from the study of the double reciprocal plot and the kinetic constants were determined both graphically and with STATISTICA ’99 Edition (Tulsa, OK, USA). As shown in Figure 4.7, the double reciprocal curves intersected in the second quadrant, revealing that, at increasing AMI concentration, the affinity of BTCh for the enzyme (K_s) increased proportionally, whilst the V_m decreased. This behavior is a classic trend for linear mixed–type inhibition (partially competitive and pure noncompetitive). The values of K_s and V_m are displayed in Table 2. In order to obtain a clear understanding of which of the mixed–type inhibition components predominates over the other, the secondary plot of Lineweaver–Burk was made from the slope and intercept of the primary double reciprocal plot and kinetic constants, K_i and αK_i were estimated graphically (Fig. 4.8). Using the same data obtained from the inhibitory kinetic studies, the Dixon plot was also generated by plotting the reciprocal of specific activity against the inhibitor concentrations (0.25 μM, 0.5 μM, 1 μM, 2 μM, 4 μM and 8 μM) from the region of linearity. From the point of intersection of the curves in the second quadrant, K_i was graphically estimated as well. Since we could not obtain a clear understanding of which of the mixed–type inhibition components predominates over the other, the secondary replot of Dixon (Fig. 4.10; 4.11) was generated from the data extracted from the primary Dixon plots.

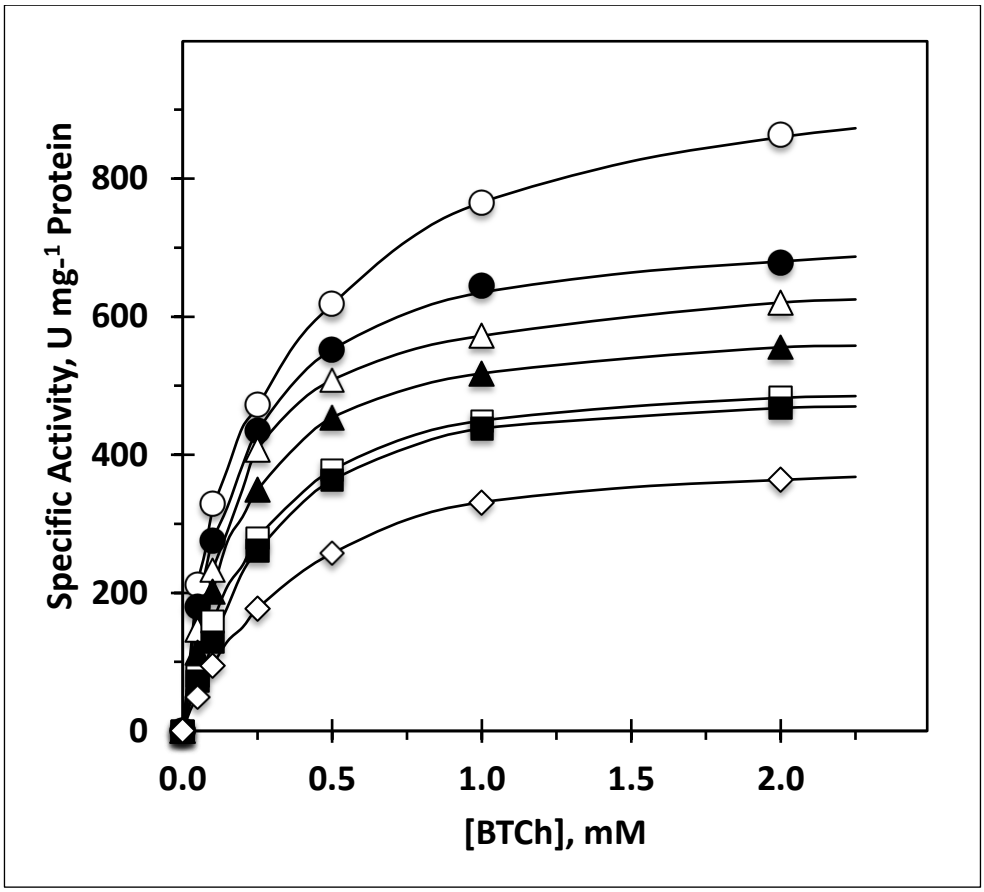

Figure 4.6. Inhibition of the BChE-catalyzed hydrolysis of BTCh by AMI. The graph illustrates Michaelis–Menten plot in the absence (control) and in the presence of AMI. Each data point is the average of three different absorbance readings. ○, control ; [AMI]: ●, 0.25 μM; △, 0.5 μM; ▲, 1 μM; □, 2 μM; ■, 4 μM; ◇, 8 μM.

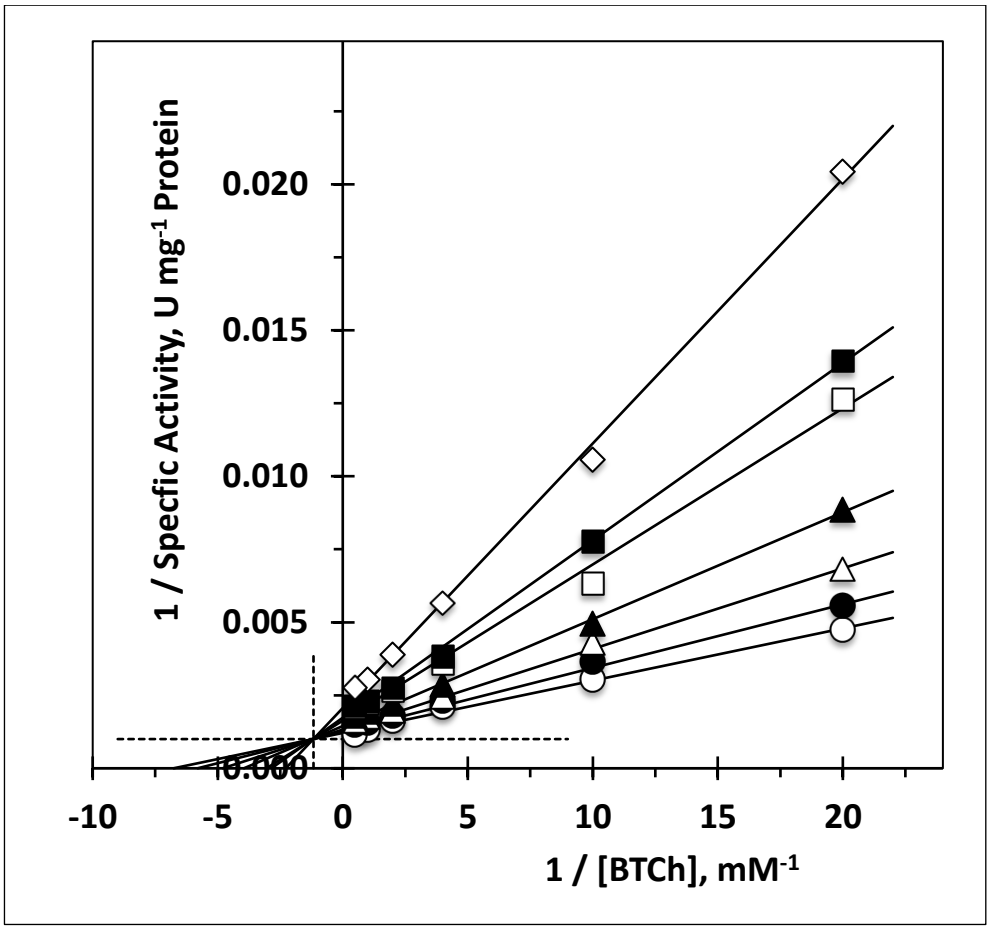

Figure 4.7. Inhibition of the BChE-catalyzed hydrolysis of BTCh by AMI. The graph illustrates Lineweaver–Burk plot in the absence (control) and in the presence of AMI. Each data point is the average of three different absorbance readings. ○, control ; [AMI]: ●, 0.25 μM; △, 0.5 μM; ▲, 1 μM; □, 2 μM; ■, 4 μM; ◇, 8 μM.

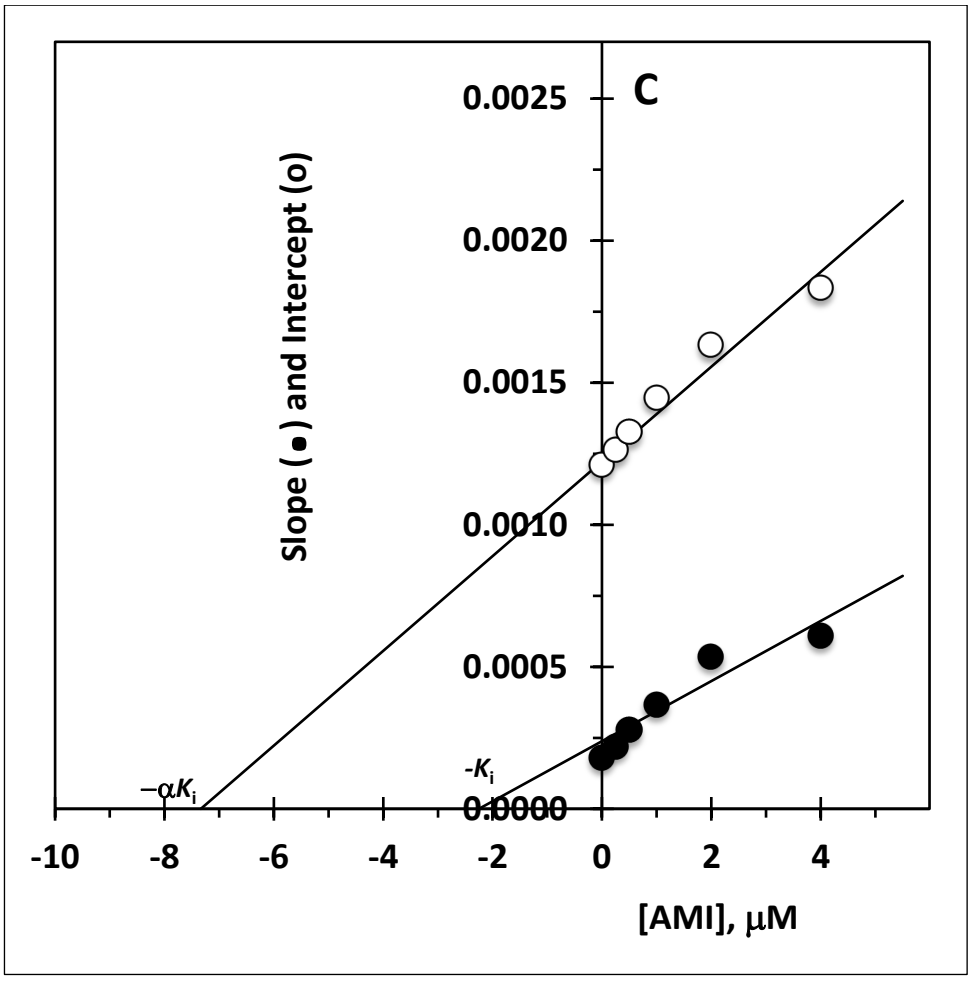

Figure 4.8. Lineweaver–Burk secondary replot of intercept and slope against [AMI]. Each data point is an average of three determinations.

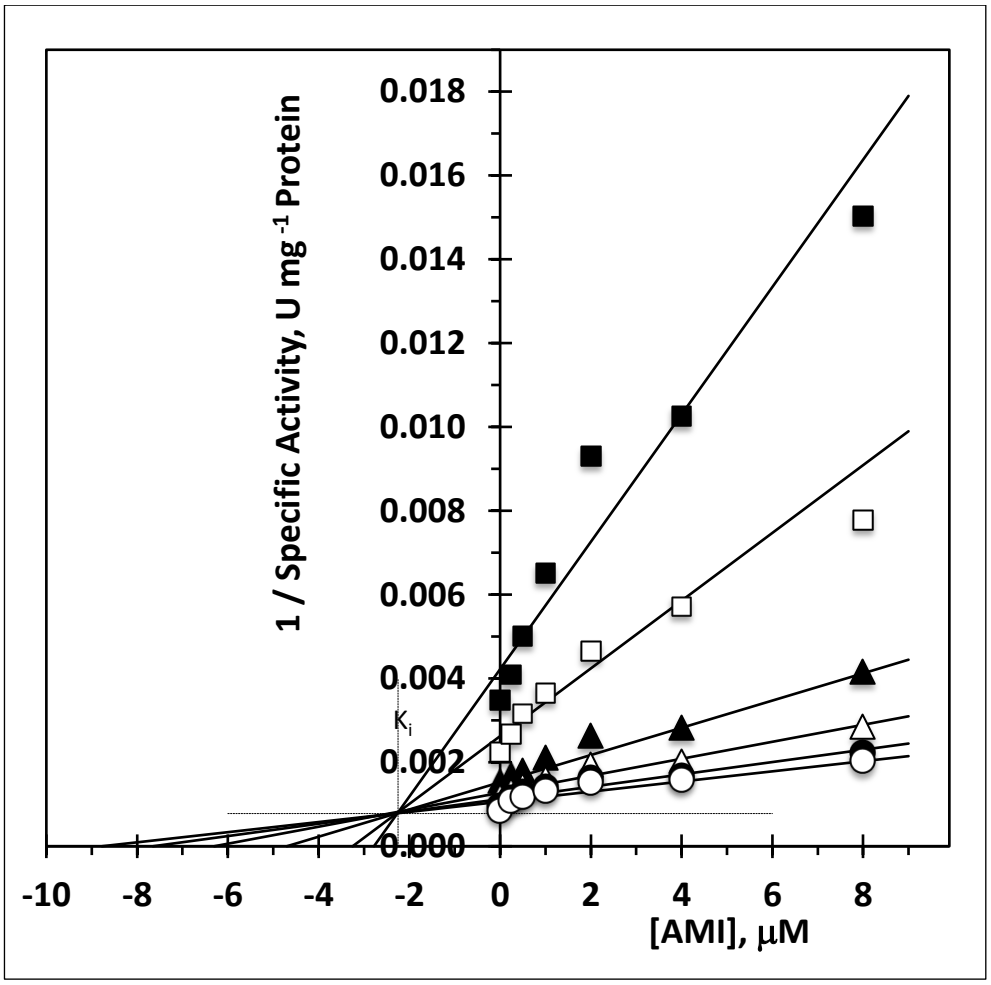

Figure 4.9. Dixon plot for the inhibition of equine serum BChE by AMI. The ordinate is the reciprocal of the specific activity of BTCh hydrolysis expressed in U mg^{-1} protein and the abscissa is [AMI]. [BTCh]: ■, 0.05 mM; □, 0.1 mM; ▲, 0.25 mM; △, 0.5 mM; ●, 1.0 mM; ○, 2.0 mM.

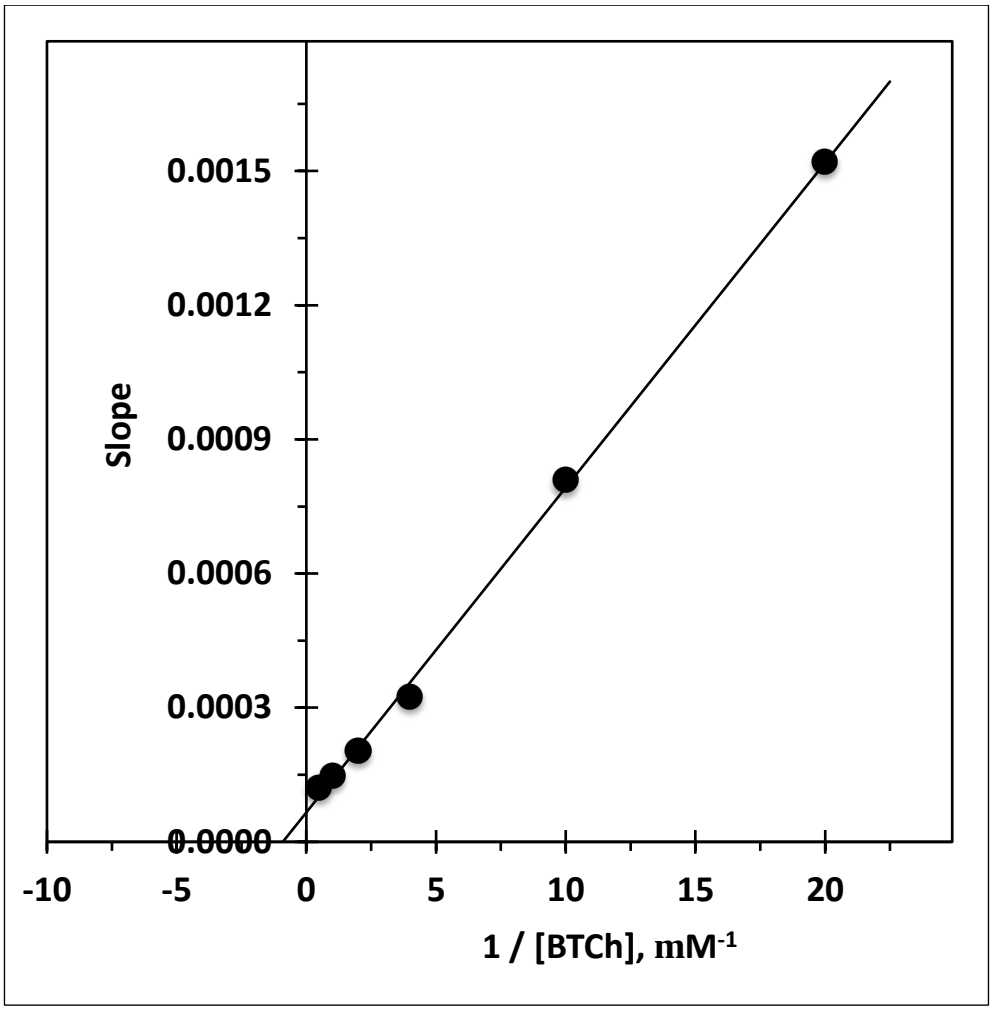

Figure 4.10. Secondary plot of Dixon: slope values from Dixon plot versus reciprocal of BTCh concentrations. Each data point is an average of three determinations.

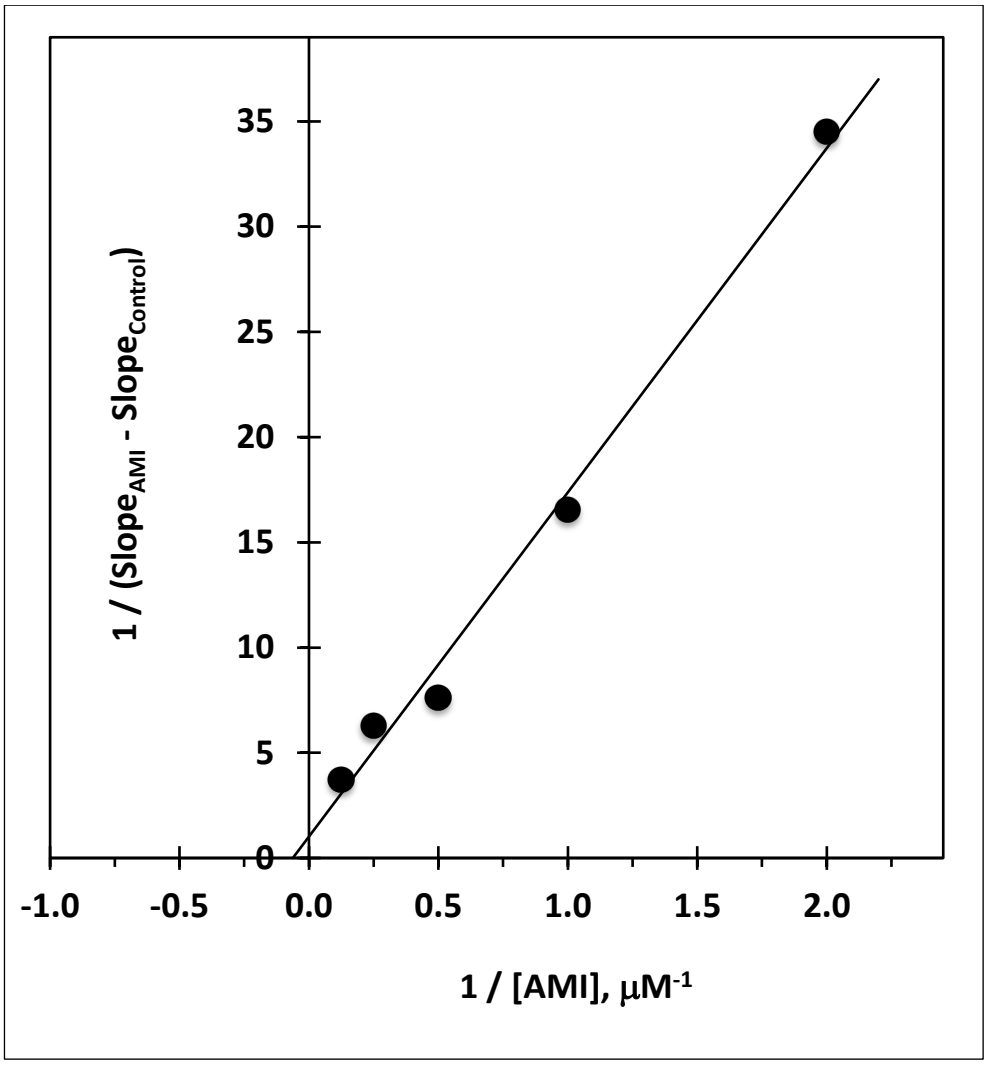

Figure 4.11. Secondary plot of Dixon: reciprocal of slope values from Dixon plot versus reciprocal of AMI concentrations. Each data point is an average of three determinations.

Table 2. Kinetic Parameters for the Inhibition of Butyrylcholinesterase by Amitriptyline

Parameters	Values
V_m	1070 ± 28 U mg^{-1} protein
α	3.26 ± 1.52
K_i	2.25 ± 0.66 μM
αK_i	7.34 ± 1.0 μM
K_s	0.169 ± 0.019 mM

Values were calculated using STATISTICA ’99 Edition (Tulsa, OK, USA). The behavior of BChE was found to conform to Hooke-Jeeves Pattern Moves.

4.4. Homology Modeling

Amino acid sequence alignment between the target sequence (eqBChE) and template sequence (huBChE) indicated 90.4 % sequence identity over 574 residues (Table 3). After the target-template alignment, the sequence alignment and template structure was used to build a structural model of eqBChE. Table 3 displays the eqBChE amino acid sequence.

Table 3. Amino Acid Sequence of Equine Serum Butyrylcholinesterase

EEDIIITTKNGKVRGMNLPVLGGTVTAFLGIPYAQPPLGRLRFKKPQSLTKWSNIWNATK
YANSCYQNTDQSFPGFLGSEMWNPNTELSEDCLYLNVWIPAPKPKNATVMIWIYGGGFQT
GTSSLPVYDGKFLARVERVIVVSMNYRVGALGFLALSENPEAPGNMGLFDQQLALQWVQK
NIAAFGGNPRSVTLFGESAGAASVSLHLLSPRSQPLFTRAILQSGSSNAPWAVTSLYEAR
NRTLTLAKRMGCSRDNETEMIKCLRDKDPQEILLNEVFVVPYDTLLSVNFGPTVDGDFLT
DMPDTLLQLGQFKRTQILVGVNKDEGTAFLVYGAPGFSKDNNSIITRKEFQEGLKIFFPR
VSEFGRESILFHYMDWLDDQRAENYREALDDVVGDYNIICPALEFTRKFSELGNDAFFYY
FEHRSTKLPWPEWMGVMHGYEIEFVFGLPLERRVNYTRAEEILSRSIMKRWANFAKYGNP
NGTQNNSTRWPVFKSTEQKYLTLNTESPKVYTKLRAQQCRFWTLFFPKVLELTGNIDEAE
REWKAGFHRWNNYMMDWKNQFNDYTSKKESCSDF

Table 4. Amino acid sequence alignment of equine and human Butyrylcholinesterase

```
SP|P06276| MHSKVTIICIRFLFWFLLLCMLIGKSHTEDDIIIATKNGKVRGMNLTVFGGTVTAFLGIP 60
SP|P81908| ----------EEDIIITTKNGKVRGMNLPVLGGTVTAFLGIP 32
                     *.****.********** *.**********

SP|P06276| YAQPPLGRLRFKKPQSLTKWSDIWNATKYANSCCQNIDQSFPGFHGSEMWNPNTDLSEDC 120
SP|P81908| YAQPPLGRLRFKKPQSLTKWSNIWNATKYANSCYQNTDQSFPGFLGSEMWNPNTELSEDC 92
          **********.********** ** ******* *********.*****

SP|P06276| LYLNVWIPAPKPKNATVLIWIYGGGFQTGTSSLHVYDGKFLARVERVIVVSMNYRVGALG 180
SP|P81908| LYLNVWIPAPKPKNATVMIWIYGGGFQTGTSSLPVYDGKFLARVERVIVVSMNYRVGALG 152
          **********.********** **********

SP|P06276| FLALPGNPEAPGNMGLFDQQLALQWVQKNIAAFGGNPKSVTLFGESAGAASVSLHLLSPG 240
SP|P81908|  FLALSENPEAPGNMGLFDQQLALQWVQKNIAAFGGNPRSVTLFGESAGAASVSLHLLSPR 212
          ****  **********.**********

SP|P06276| SHSLFTRAILQSGSFNAPWAVTSLYEARNRTLNLAKLTGCSRENETEIIKCLRNKDPQEI 300
SP|P81908| SQPLFTRAILQSGSSNAPWAVTSLYEARNRTLTLAKRMGCSRDNETEMIKCLRDKDPQEI 272
          *: ********** **********.***  ****.****.*****.******

SP|P06276|  LLNEAFVVPYGTPLSVNFGPTVDGDFLTDMPDILLELGQFKKTQILVGVNKDEGTAFLVY 360
SP|P81908| LLNEVFVVPYDTLLSVNFGPTVDGDFLTDMPDTLLQLGQFKRTQILVGVNKDEGTAFLVY 332
          ****.*****.* ********** **.*****.**********

SP|P06276| GAPGFSKDNNSIITRKEFQEGLKIFFPGVSEFGKESILFHYTDWVDDQRPENYREALGDV 420
SP|P81908| GAPGFSKDNNSIITRKEFQEGLKIFFPRVSEFGRESILFHYMDWLDDQRAENYREALDDV 392
          ********** *****.******* **.**** *******.**

SP|P06276| VGDYNFICPALEFTKKFSEWGNNAFFYYFEHRSSKLPWPEWMGVMHGYEIEFVFGLPLER 480
SP|P81908|   VGDYNIICPALEFTRKFSELGNDAFFYYFEHRSTKLPWPEWMGVMHGYEIEFVFGLPLER 452
           *****.*********.**** **.**********.**********

SP|P06276| RDNYTKAEEILSRSIVKRWANFAKYGNPNETQNNSTSWPVFKSTEQKYLTLNTESTRIMT 540
SP|P81908| RVNYTRAEEILSRSIMKRWANFAKYGNPNGTQNNSTRWPVFKSTEQKYLTLNTESPKVYT 512
          * ***.**********.************* ****** ********** :: *

SP|P06276|KLRAQQCRFWTSFFPKVLEMTGNIDEAEWEWKAGFHRWNNYMMDWKNQFNDYTSKKESCV 600
SP|P81908|KLRAQQCRFWTLFFPKVLELTGNIDEAEREWKAGFHRWNNYMMDWKNQFNDYTSKKESCS 572
          ********** *******.******** ******************************

SP|P06276| GL 602
SP|P81908| DF 574
```

(*****) indicates positions which have single or fully conserved residues. (**:**) indicates conservation between groups of strongly similar properties. (**.**) indicates conservation between groups of weakly similar properties. sp_p06276_CHLE_human 100.00 90.4. sp_P81908_CHLE_equine 90.4 100.00 query= Sequence Template= 3O9M.A Id= 90.4 Qlen= 602 Model_len= 574. Amino acid residues in red indicate the catalytic triads.

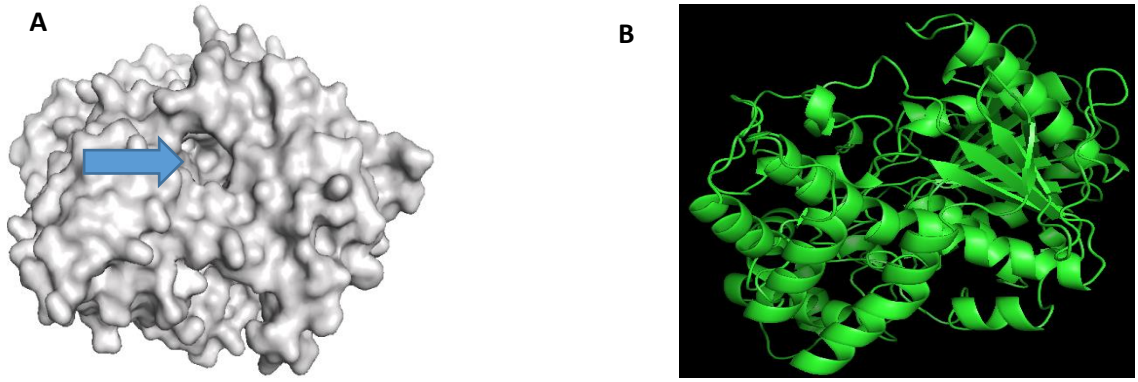

Fig 4.12A & B. Homology models of eqBChE based on a huBChE template. The arrow on Fig. 14A points to the active-site gorge. Visualized with PyMOL (The PyMOL Molecular Graphics System, Schrödinger LCC, open source v.1.2x. http://www.pymol.org).

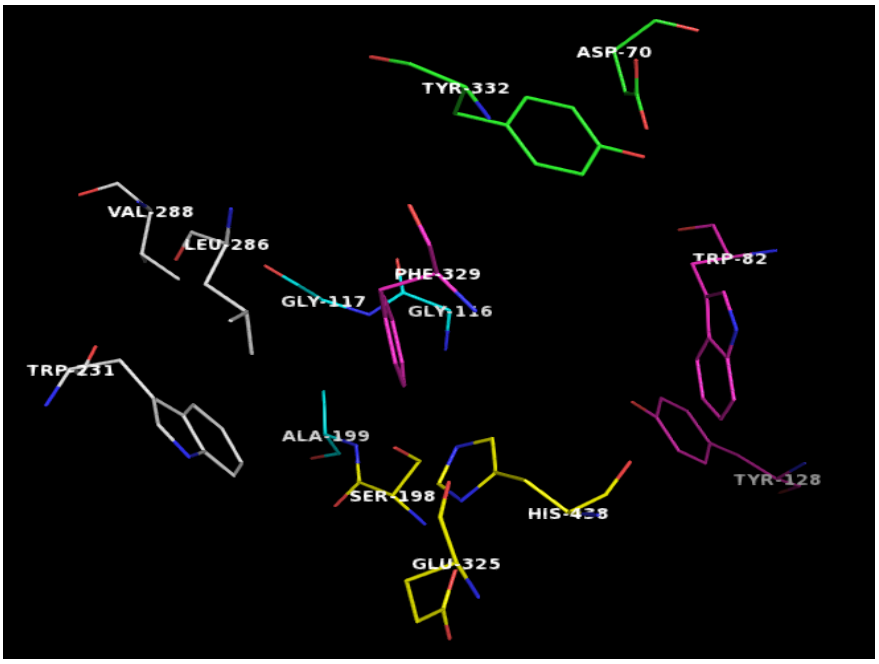

Fig 4.13. Close up view of BChE active-site gorge key residues. Drawn with PyMOL (The PyMOL Molecular Graphics System, Schrödinger LCC, open source v.1.2x. http://www.pymol.org).

4.5. Binding of Amitriptyline to Butyrylcholinesterase

In order to delineate the binding mode of AMI with BChE, a molecular docking approach was employed. The outcome indicated that AMI docked itself in the active site gorge of eqBChE, forming hydrophobic interactions with Leu286, Val288, Trp231, Phe329 and Tyr332. Phe329 and Tyr231 formed π–π stacking interaction whilst the tertiary amine ligand group formed a salt bridge (Figure 4.14; 4.15). Table 5 enumerates the interactions of AMI and BChE.

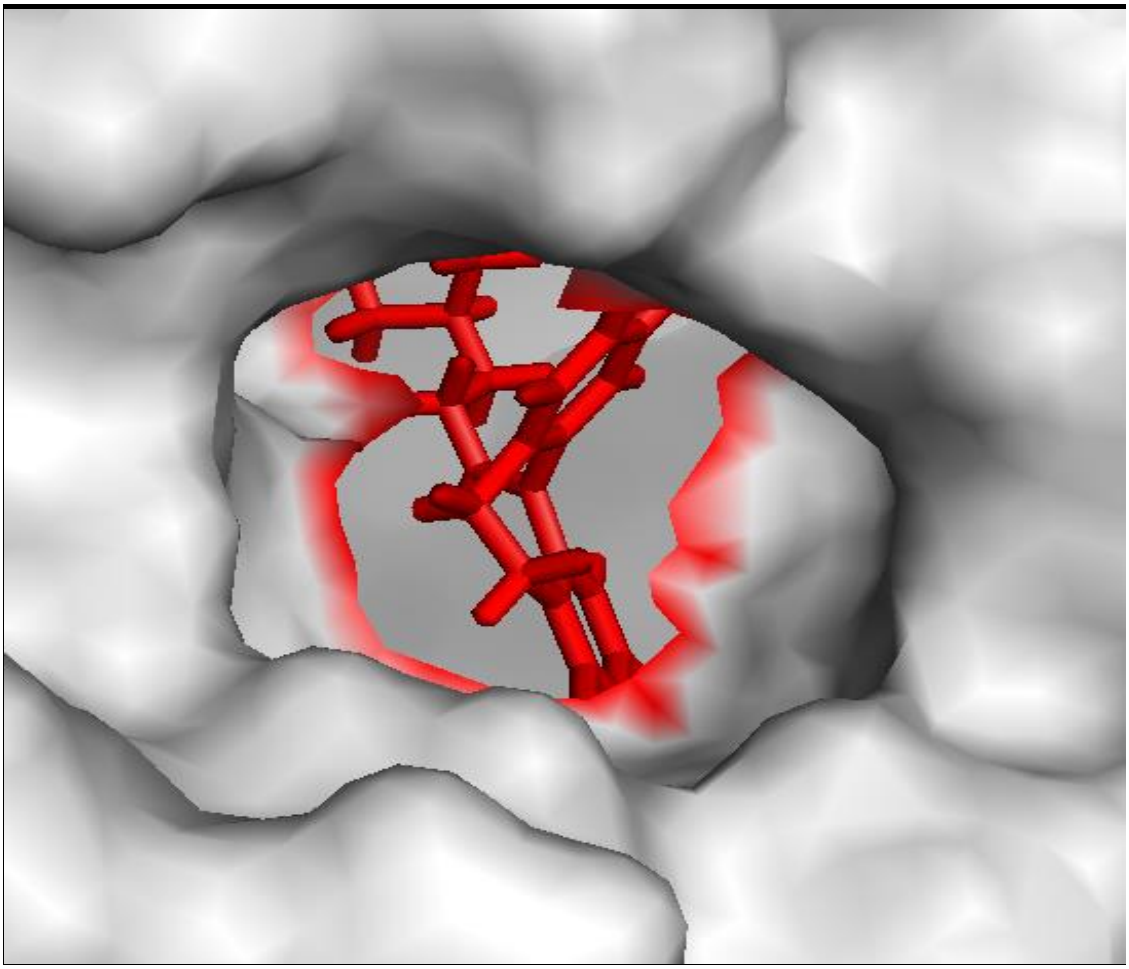

Fig 4.14 shows the active site gorge of BChE with bound AMI. Drawn with PyMOL (The PyMOL Molecular Graphics System, Schrödinger LCC, open source v.1.2x. http://www.pymol.org).

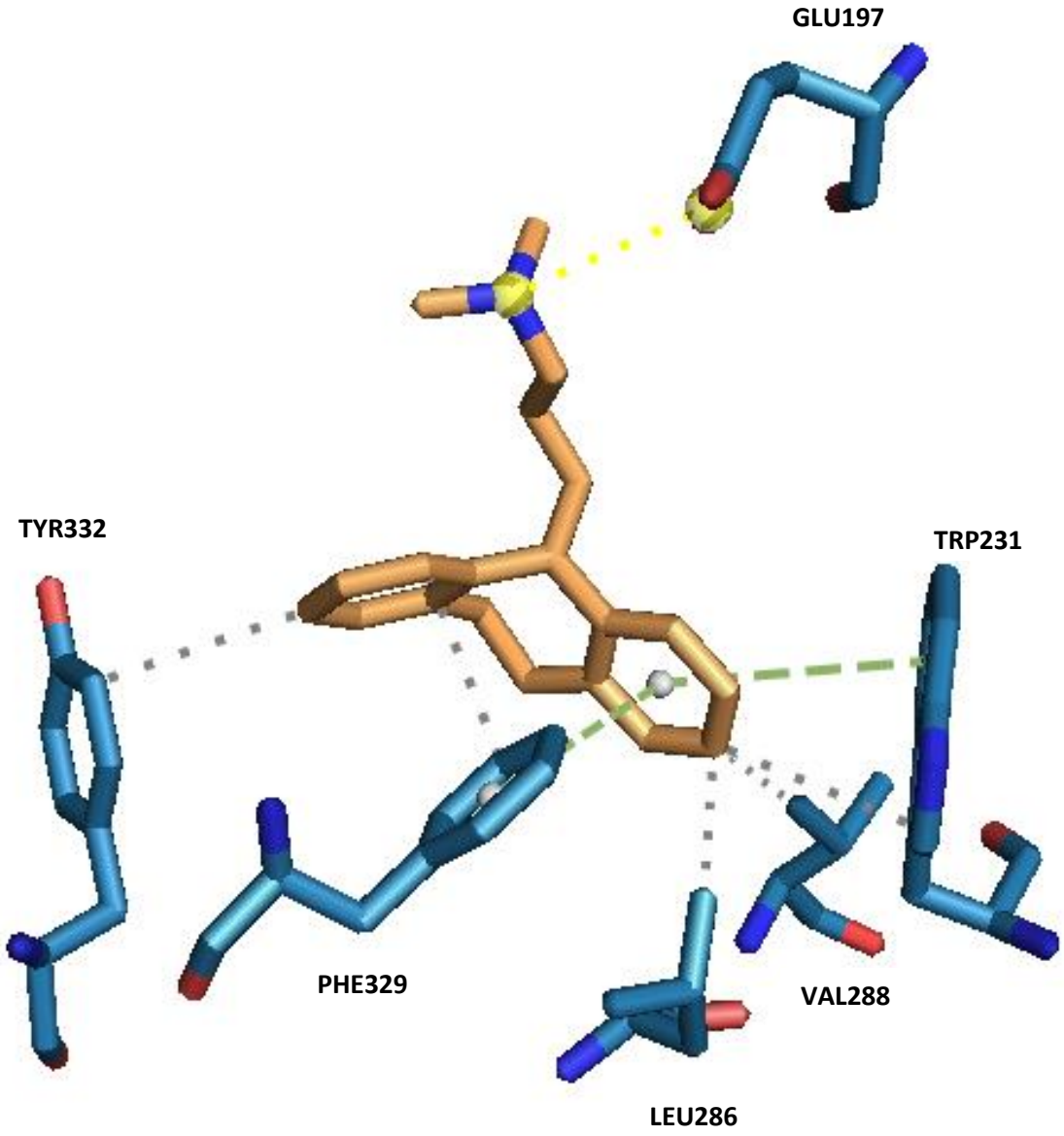

Fig 4.15 reveals amino acid residues that interacts with different units of AMI when the inhibition is of a partially competitive nature. Image generated using PLIP (Salentin *et al.*, 2015)

Table 5. Relatively strong Competitive Binding Interaction Profile for Amitriptyline

ΔG(kcal)	Residue	Interacting Subsite	Interaction Type	Distance(Å)
-2.29	Glu 197	CBS*	Salt bridge	4.11
	Trp 231	ABP**	Hydrophobic	3.95
	Trp 231	ABP**	л Stacking	4.81
	Leu 286	ABP**	Hydrophobic	3.39
	Val 288	ABP**	Hydrophobic	3.47
	Phe 329	E-helix	Hydrophobic	3.68
	Phe 329	E-helix	л Stacking	5.30
	Tyr 332	PAS***	Hydrophobic	3.99

* Choline Binding Site ** Acyl Binding Pocket ***Peripheral Anionic Site

4.6 Superimposition of Butyrylthiocholine and Amitriptyline

When AMI was superimposed with BTCh inside the active site gorge of butyrylcholinesterase, the observation made was quite revealing. According to Illanes *et al*, in partial competitive inhibition the inhibitor interferes with the substrate without completely excluding it from the active site (Illanes *et al,* 2008). From fig. 4.16, a steric clash could indeed be gleaned from the superimposition of AMI and BTCh, however it seems highly unlikely that this steric disturbance could displace BTCh from the active site gorge, especially at low AMI concentration. That said, substrate hydrolysis could possibly have been hampered as access of BTCh to the esteratic site could be blocked. This is in line with the strong mixed-type partially competitive component AMI exudes.

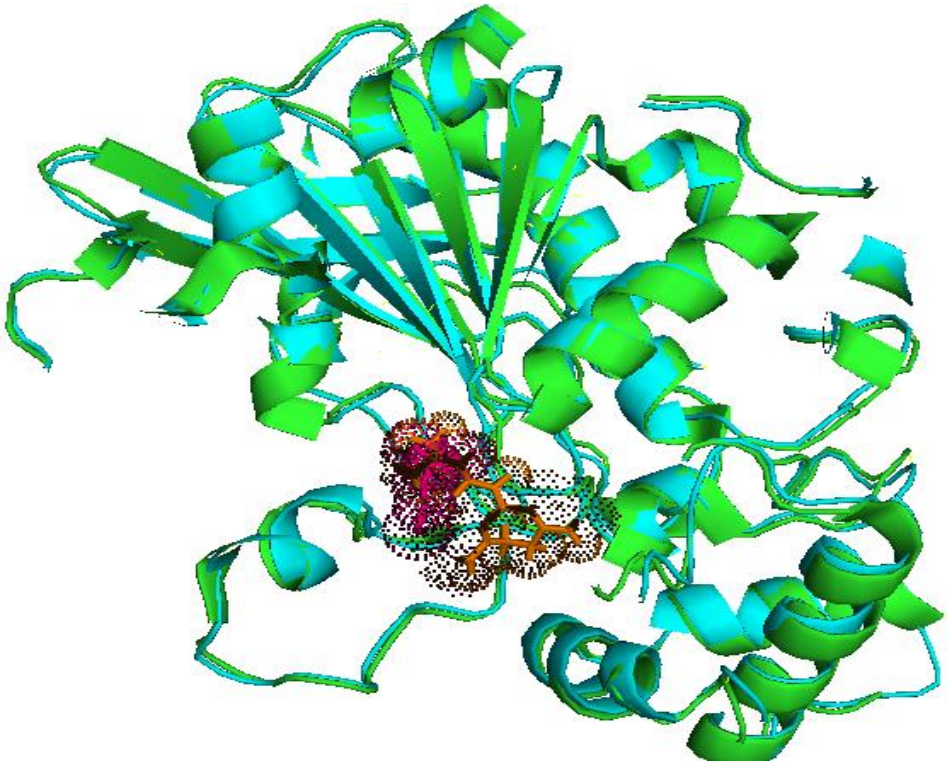

Fig. 4.16. Superimposition of BTCh and AMI inside the active site gorge of BChE. BTCh is colored pink whilst AMI is colored orange. Drawn with PyMOL (The PyMOL Molecular Graphics System, Schrödinger LCC, open source v.1.2x. http://www.pymol.org).

4.7 Binding of both Amitriptyline and Butyrylthiocholine inside the Active Site of Butyrylcholinesterase

Both AMI and BTCh were docked inside the active site gorge of BChE with the aim of delineating the binding mode of AMI of in the presence of BTC. The outcome showed that AMI docked itself at the peripheral anionic site of eqBChE, establishing a salt bridge and a hydrophobic interaction with Asp70, and yet another hydrophobic interaction with Tyr332. Meanwhile, BTCh formed hydrophobic interactions with Leu328, Phe329, Tyr332, a π–cation interaction with Trp82 and a salt bridge with Glu197. (Figure 4.17A and Figure 4.17B). Table 6 enumerates the interactions of BTCh inside BChE's active site gorge. Fig. 4.18 illustrates the interaction of AMI with key PAS residues (Asp70 and Tyr 332) responsible for its mixed-type noncompetitive component while Table 7 enumerates the various types of interaction it undergoes.

A

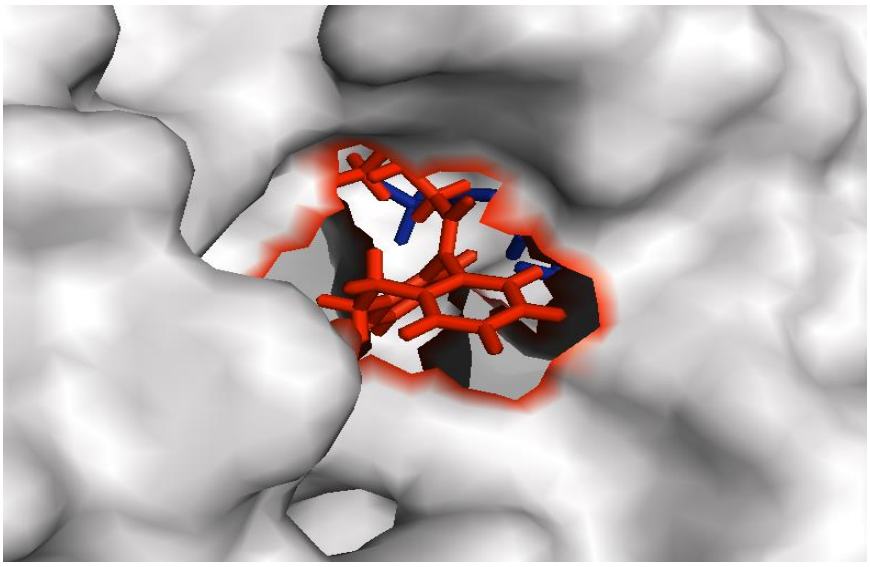

Fig. 4.17. **A** shows AMI and BTCh squeezed together inside the BChE active site gorge. AMI is colored red while BTCh is colored blue. Drawn with PyMOL (The PyMOL Molecular Graphics System, Schrödinger LCC, open source v.1.2x. http://www.pymol.org).

B

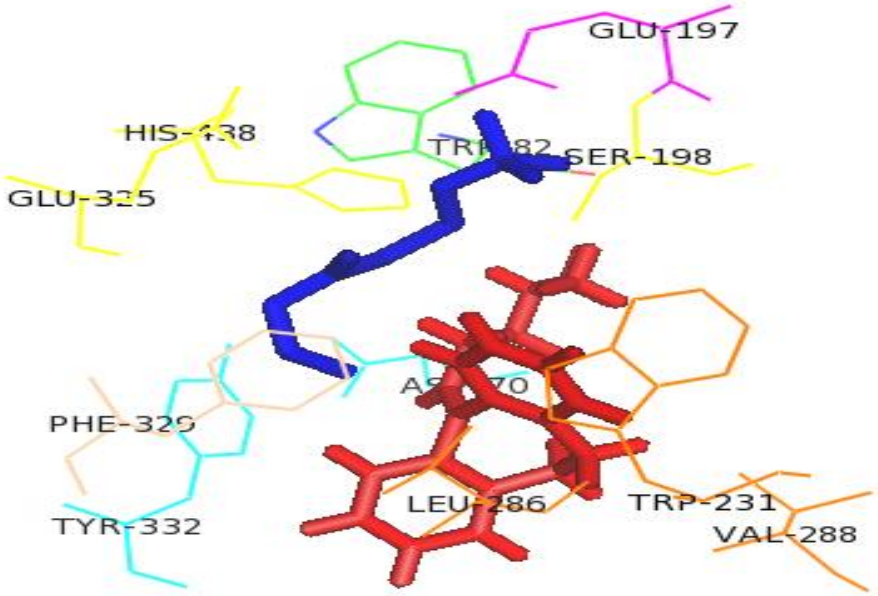

Fig. 4.17. **B** is the interaction profile of both AMI and BTCh inside BChE active site gorge, with AMI interacting with PAS residues. AMI is colored red while BTCh is colored blue. Drawn with PyMOL (The PyMOL Molecular Graphics System, Schrödinger LCC, open source v.1.2x. http://www.pymol.org).

Table 6. Binding Interaction Profile for BTCh

Residue	Interacting Subsite	Interaction Type	Distance (Å)
Trp 82	CBS***	π- Cation	4.32
Glu 197	CBS***	Salt-bridge	4.17
Tyr 332	PAS**	Hydrophobic	3.75
Ala 328	ABP*	Hydrophobic	3.96
Phe 329	E-helix	Hydrophobic	3.64

* Acyl Binding Pocket **Peripheral Anionic Site ***Choline Binding Site

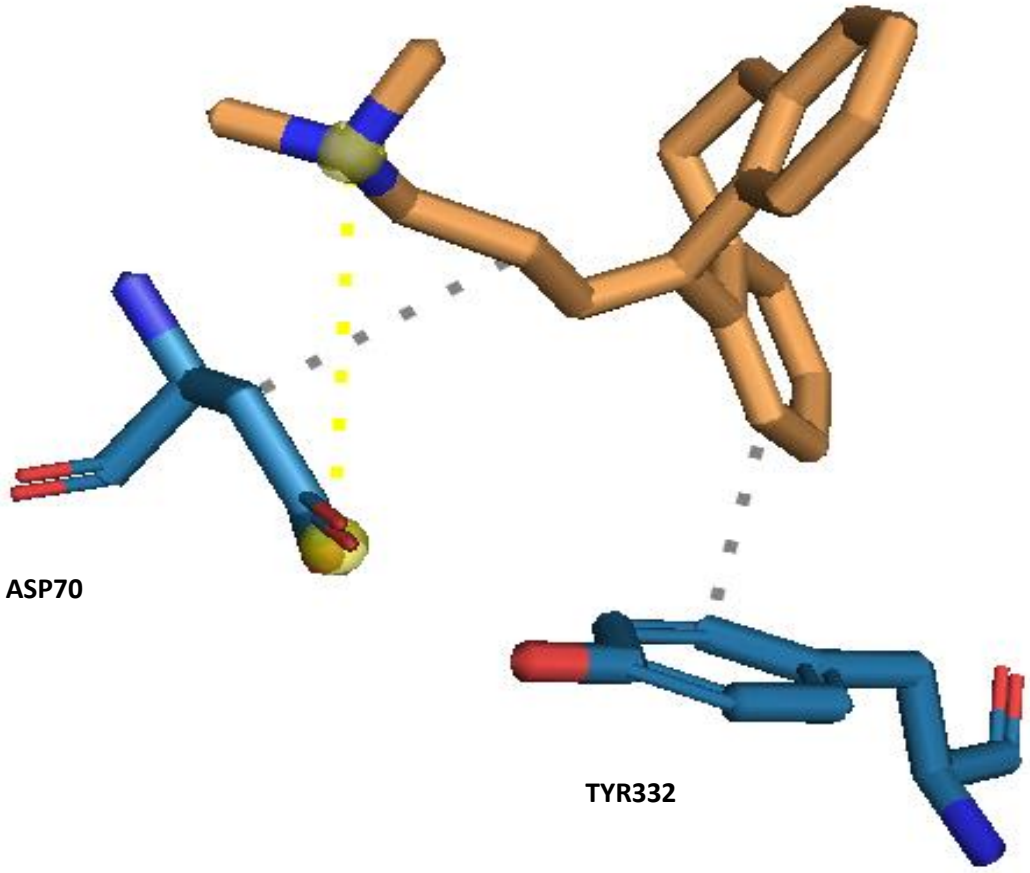

Fig 4.18 reveals amino acid residues that interacts with different units of AMI when the inhibition is of a noncompetitive nature. Image generated using PLIP (Salentin *et al.*, 2015).

Table 7. Noncompetitive Binding Interaction Profile for Amitriptyline

Residue	Interacting Subsite	Interaction Type	Distance (Å)
Asp 70	PAS*	Salt-bridge	5.28
Asp 70	PAS*	Hydrophobic	3.96
Tyr 332	PAS*	Hydrophobic	3.02

*Peripheral anionic site

5. DISCUSSION

There is at least one fresh case of Alzheimer disease every seven seconds in the world (Massoud and Gauthier, 2010). According to Greig *et al*. BChE has been a neglected target, for a long time, in anti-AD disease drug discovery, as it seems to have an unclear physiological role besides being localized in the "wrong" areas of the human brain (Greig *et al*., 2005). However, alterations that take place in the AD brain has called for a re-evaluation of the function of BChE, and it is presumed that inhibitors of BChE may provide a new approach towards the treatment of AD (Giacobini, 2004; Greig *et al*., 2005; Lane *et al*., 2006).

In this study, the focus was to investigate the kinetic behavior of BChE purified from equine serum under the influence of the tricyclic antidepressant, amitriptyline (AMI). The possible molecular grounds for understanding their interaction were also explored. AMI is a dibenzocycloheptadiene derivative. Mc Kenna *et al*. reported that an increased inhibitory activity on BChE was observed when substituents were added to the tricyclic ring structure of tacrine (Mc Kenna *et al*., 1997). AMI and tacrine derivatives have structural similarities. At 125 μM concentration, AMI exhibited strong activity against BChE by causing 90.7% inhibition with an IC_{50} value of 10 μM (Fig. 4.3). Muller *et al.* reported an IC_{50} value of 9.43 μM for AMI against BChE from human serum. Hence, with an IC_{50} of 10 μM for AMI against BChE purified from equine serum, the present study could be said to be in accord with that of Muller *et al.* (Muller *et al.,* 2002).

Previously, a research work by Cokugras and Tezcan suggested that AMI possibly binds to BChE active site in a partially competitive manner (Cokugras and Tezcan, 1997). In order to elucidate the kinetic mechanism of inhibition in the present work, the activity of the enzyme was determined at varied substrate (BTCh) and inhibitor (AMI) concentrations. The Lineweaver-Burk plot (Fig. 4.7) displayed convergent curves in the second quadrant. Generally, this finding presupposes that binding of AMI and BTCh is not mutually exclusive; and that AMI could potentially bind simultaneously to the enzyme substrate complex within the BChE active site gorge in a partially competitive manner (Fig. 4.14) as well as to the peripheral anionic site in a pure noncompetitive mode (Fig. 4.17) in line with the nature of linear mixed-type inhibition. In the secondary replots of

the double reciprocal, linear plots were obtained (Fig. 4.8). This made it difficult to distinguish between the relative prevalence of the two components; by reason that the secondary replots of Lineweaver-Burk is a linear function of the inhibitor concentration in both cases. However, this challenge was overcome with Dixon replots (Figure 4.10; 4.11) in which the straight line virtually passed through the origin, suggesting a pronounced competitive component (Segel, 1975). To validate this, the experimental data was fitted to the Hooke-Jeeves pattern moves. And, whilst the V_m was found to be 1070 ± 28 U mg^{-1} protein, it was observed that the α-value by which the substrate binding affinity was altered when AMI bound to BChE was 3.26 ± 1.52. The results further revealed that the inhibitor bound to the free enzyme with the inhibition constant (K_i) of 2.25 ± 0.6 μM. The dissociation constant (αK_i) for the association of the inhibitor (AMI) with the enzyme substrate (BChE–BTCh) complex was found to be 7.34 ± 1 μM, indicating that the inhibitor caused about 3.26-fold reduction in the affinity of the enzyme for the substrate (Table 2). This observation runs in concert with the increase in substrate binding affinity (K_s) from 0.169 ± 0.019 μM to 0.551 ± 0.029 μM in the presence of AMI. The inhibition of BChE by AMI suggests a phenomenon where both the enzyme (E) and the enzyme-inhibitor (EI) complex bound, although with different affinities, to the substrate (S). It was found that the E has a higher affinity for the S than the EI complex has for the same S. Once AMI remains bound, a certain amount of the enzyme will subsist in the nonproductive enzyme-substrate-inhibitor (ESI) complex. This results in decreased V_m. And since some portion of the enzyme free for association with the substrate remains in the EI complex at any I concentration, K_s ultimately increased by a factor of α (3.26±1.52). However, at unlimited AMI concentration, BChE is moved into the EI and ESI mode. But because the ESI complex is nonproductive, the reaction velocity is consequently driven to zero by increasing amitriptyline concentration. This is the normal trend for mixed-type competitive.

Lately, several studies have shown the importance of sequence comparison and molecular modeling in delineating the function of specific amino acids in binding of inhibitors or substrates to enzymes. So, in an attempt to validate the kinetic studies and obtain a better understanding of BChE inhibition, homology modeling and molecular docking study was

carried out to profile the interaction of AMI in the BChE active site. Due to the lack of an available X-ray crystal structure for eqBChE, modeling studies with eqBChE made use of a generated model (Fig. 4.12) using huBChE as template. This model was generated on ground of the 90.4% sequence identity (no disparities between the key amino acid residues within their active sites) observed between the eqBChE and huBChE when homology modeling was conducted (Table 4).

Docking study of amitriptyline was subsequently performed using the modeled eqBChE and the results were analyzed taking into consideration the docking energy score. SwissDock generated 250 docking solutions. The docking cluster with the lowest estimated binding energy was selected. The top docking solution SwissDock generated exhibited interaction pattern characteristic of other amitriptyline docked complexes, like the crystal structure of the A variant of human alpha 1 acid glycoprotein and amitriptyline complex (3APV) and the crystal structure-based design and discovery of novel PARP1 anti-agonist (BL-PA10) that induces apoptosis and inhibit metastasis in triple negative breast cancer (5HA9). In each of the aforementioned complexes that had amitriptyline bound, the main interactions were hydrophobic, π–π stacking and salt-bridge. Similar association pattern was observed in the top docking solution of BChE–AMI complex. The rest of the docking solutions SwissDock produced displayed mainly hydrophobic interactions. Mixed–type Inhibitor compounds generally consist of cyclic moieties linked to a side chain of several lengths and as a result occupy large volumes (Maja *et al*., 2010). AMI is obviously a planar structure and the docking studies depicted its gorge spanning nature. Figure 4.14 shows the orientation and conformation of AMI inside the active site gorge of BChE. In agreement with the kinetic studies, when the docking study was performed, AMI was found to extend from the peripheral anionic site where its C-11 transiently made hydrophobic interaction with Tyr332, to the E-helix where another hydrophobic association took place between C-9 of AMI and Phe329 of BChE; and eventually accommodated at the bottom of the BChE active site gorge where the C-4 of its aromatic ring established multiple hydrophobic interactions with amino acid residues Leu286, Val288 and Trp231. Besides the rich network of hydrophobic interactions, there was also a л–л interaction between the aromatic ring of AMI and Trp231. These

hydrophobic and л–л stacking associations of the tricyclic moiety of AMI at the acyl binding-pocket just at the neighborhood of the esteratic site could make the acylation-desacylation difficult, and this would culminate in a decrease in BChE activity. These interactions might as well eventually engender steric clashes between the residues that constitute the BChE active site gorge. The docking outcome equally revealed that the basic tertiary amine ligand group of AMI interacted favorably with Glu197. Glu197 is positioned next to the Ser198 of the catalytic triad. The distance of the ternary ammonium nitrogen of AMI side chain from the Glu197 carbonyl atom was 4.11 Å. However this electrostatic interaction could not be said to be unique or account for any huge role in the binding of the ligand to BChE. Also just like AMI, the substrate also had a temporary association with Tyr332. But this could not be said to have impacted on substrate binding, given that it is a characteristic trend for ligands to associate with Tyr332 before sliding into the gorge. Most significantly however, the planar mode of the aryl moiety in AMI might have constituted a major factor in hampering the accessibility of substrate to the acylation site where the catalytic triad is located. Also, the putative л–л interaction between the aromatic rings of AMI and the ABP residue Trp231 and Phe329 of the E-helix seemed highly favored since there is no any indication whatsoever that AMI reached and reacted with Ser198 of the catalytic triad. One factor that perhaps facilitated BChE–AMI л-л stacking could be attributed to the 'butterfly' nature of the AMI tricycle. So, the inhibition of BChE by AMI could be said to have involved a strong interaction of the AMI aromatic ring with Phe329 and Trp231. The potency of the inhibition could equally be attributable to side chain of AMI that projected into the active site gorge. These interactions possibly stabilized the binding of the AMI and allowed the tertiary amine ligand group to point towards the catalytic triad. In addition to interfering with substrate binding, recall that AMI established a transient association with Tyr332 of the PAS. Phe329 and Tyr332 constitute the helical polypeptide portion that contains Glu325 of the catalytic triad (E-helix, Figure 2.6) and this could engender conformational changes within the triad, and that by itself could trigger a negative effect on substrate hydrolysis. This essentially would result in a non-productive enzyme inhibitor substrate complex within the active site gorge, and ultimately decreasing the catalytic turnover of BChE. These observations could be said to agree with the proposition of Saxena *et al.* that reversible

inhibition occasioned by tricyclic compounds are mostly due to their л-л interaction with Phe329 and Tyr332 above the BChE active site gorge's catalytic triads (Saxena *et al.*, 1997). Essentially, it could be surmised that the preponderance of mixed-type competitive inhibition nature of AMI against BChE might augment acetylcholine level in brain of AD patients and ultimately contribute towards improved cognitive function.

But one sore point remains! BChE has been implicated in the formation and deposition of neurotoxic Aβ plaques inside its PAS. The existence of the PAS appears to be essential in BChE's role of promoting Aβ aggregation. To highlight the importance of PAS–AMI interaction, docking studies subsequently showed that in the presence of docked BTCh, AMI effectively docked itself and spanned the periphery of the active site gorge of eqBChE (Fig. 4.17B), forging hydrophobic interaction and salt-bridge with Asp70, a key PAS residue; and another hydrophobic interaction with PAS residue Tyr332 (Fig. 4.18). These interactions ultimately accounted for the subtle noncompetitive nature of the mixed-type inhibition. The import of this finding is that, possibly at infinite substrate concentration, the noncompetitive component of the mixed-type inhibition becomes apparent. By associating with Aβ through the PAS, BChE induces amyloid fibrils deposit in the brain. This produces stable BChE-Aβ complexes that are even more deleterious when compared to single Aβ peptides (Masson, 1996). Aβ peptide associates with the PAS engendering a conformational change. This results in the amyloidogenic conformation and the subsequent formation of amyloid fibril culminating in the destruction of cholinergic neurons (Mesulam, 2002). Many compounds that bind to the PAS have been revealed to hinder Aβ aggregation. Prefibrillar oligomers of the Aβ are considered as possible regulator of AD pathophysiology (Diociaiuti, 2014). The deposition of Aβ plaque in AD may be triggered or even accelerated by association of Aβ with PAS. Hence, with AMI interfering with the PAS, the aggregation as well as the neurotoxic consequence of Aβ may be decreased.

Ultimately, AMI holds great potential as an anti-AD drug. This could be seen through its role in improving cognition by up-regulating the pool of ACh as a mixed-type competitive inhibitor as well as slowing the rate of Aβ induced neurodegeneration as a mixed-type noncompetitive inhibitor.

6. CONCLUSION

In the present study, the inhibitory effect of amitriptyline on equine serum butyrylcholinesterase was investigated using kinetic methods and molecular docking procedures. Overall, the outcome of the docking calculations correlated very well with the kinetic studies where it was observed that the linear mixed-type inhibition of butyrylcholinesterase by amitriptyline resulted from a predominantly competitive nature of their interaction wherein AMI possibly bound to the enzyme substrate complex, and a slightly noncompetitive component. This is even as emerging evidence suggests that AMI and other inhibitors of BChE might have an effect on the progression of AD. Given that Alzheimer's disease has to do with a loss of cholinergic neurotransmission, the availability of a drug like amitriptyline with strong effects on butyrylcholinesterase could offer an exciting prospect; however, until the clinical usefulness of AMI in cholinergic neurotransmission is proven, and the mechanism of AD progression clearly understood, it will be presumptuous to make any emphatic statement about AMI's therapeutic significance or otherwise. This is on account of the complex nature of the disease. But, beyond any other thing, this study has underscored several lines of evidence to demonstrate that BChE may perform an invaluable physiological role as far as human health and disease is concerned, besides its putative role as a bioscavenger. On account of the foregoing, it is suggested that the clinical efficacy of AMI be examined in models of memory impairment in future studies.

REFERENCES

Aaltonen, L., Syvilahti, E., Iisalo, E. and Peltomiki T. (1984) Anticholinergic activity in the serum of patients receiving maintenance amitriptyline or doxepin therapy. *Acta Pharmacol Toxicol*, 56, 75-80.

Abaut, A.Y., Chevanne, F. and Le Corre, P. (2007) Oral bioavailability and intestinal secretion of amitriptyline: Role of P-glycoprotein. *Int J Pharm*, 330(1-2), 121-128.

Abaut, A.Y., Chevanne, F. and Le Corre, P. (2009) Influence of efflux transporters on liver, bile and brain disposition of amitriptyline in mice. *Int J Pharm*, 378(1-2), 80-85.

Allderdice, P.W., Gardner, H.A.R., Galutira, D., Lockridge, O., LaDu, B.N. and McAlpine, P.J. (1991) The cloned butyrylcholinesterase (BChE) gene maps to a single chromosome site, 3q26. *Genomics*, 11, 452-454.

Anand, P. and Singh, B. (2013) A review on cholinesterase inhibitors for Alzheimer disease. *Arch Pharm Res*, 36(4), 375 – 99.

Arpagaus, M., Knott, M., Vatsis, K.P., Bartels, C.F., La Du, B.N. and Lockridge, O. (1990) Structure of the gene for human butyrylcholinesterase: evidence for a single copy. *Biochemistry*, 29, 124-131.

Asojo, O.A., Ngamelue, M.N., Homma, K. and Lockridge, O. (2011) Cocrystallization studies of full-length recombinant butyrylcholinesterase (BChE) with cocaine. *Acta Crystallographica Section F: Structural Biology and Crystallization Communications*, 67, 434-437.

Bachovchin, D.A. and Cravatt, B.F. (2012) The pharmacological landscape and therapeutic potential of serine hydrolases. *Nature Reviews Drug Discovery*, 11, 52-68.

Barcellos, C.K., Schetinger, M.R., Dias, R. D. and Sarkis, J.J. (1998) In vitro effect of central nervous system active drugs on the ATPase-ADPase activity and acetylcholinesterase activity from cerebral cortex of adult rats. *General pharmacology*, 31(4), 563-567.

Barricklow, J. and Blatnik, M. (2013) 2-Arachidonoylglycerol is a substrate for butyrylcholinesterase: A potential mechanism for extracellular endocannabinoid regulation. *Archives of Biochemistry and Biophysics*, 536(1), 1-5.

Bartels, C.F., Van der Spek, A., Lockridge, O. and La Du, B.N. (1989) A polymorphism (K-variant?) of human serum cholinesterase at nucleotide 1615, coding for Ala/Thr 539. *Federation of American Societies for Experimental Biology Journal,* 3: 741A.

Bartolini, M., Bertucci, C., Cavrini, V., and Andrisano, V. (2003) Beta-Amyloid aggregation induced by human acetylcholinesterase: inhibition studies. *Biochemical Pharmacology,* 65, 407-416.

Biberoglu, K., Schopfer, L.M., Saxena, A., Tacal, O. and Lockridge, O. (2013) Polyproline tetramer organizing peptides in fetal bovine serum acetylcholinesterase. *Biochimica et Biophysica Acta,* 1834, 745-753.

Biberoglu, K., Schopfer, L.M., Tacal, O. and Lockridge, O. (2012) The praline rich tetramerization peptides in equine serum butyrylcholinesterase *FEBS Journal,* 279(20), 3844-3858.

Birks, J. (2006) Cholinesterase inhibitors for Alzheimer's disease. *Cochrane Database of Systematic Reviews,* 1: CD005593. DOI: 10.1002/14651858.CD005593

Burch, J.E. and Hullin, R.P. (1981) Amitriptyline pharmacokinetics. A crossover study with single doses of amitriptyline and nortriptyline. *Psychopharmacol (Berl*), 74(1), 35-42.

Carolan, C.G., Dillon, G.P., Khan, D., Ryder, S.A., Gaynor, J.M., Reidy, S., Marquez, J.F., Castberg, I., Helle, J. and Aamo, T.O. (2005) Prolonged pharmacokinetic drug interaction between terbinafine and amitriptyline. *Ther Drug Monit*, 27(5), 680-682.

Chatonnet, A. and Lockridge, O. (1989) Comparison of butyrylcholinesterase and acetylcholinesterase. *Biochem J,* 260(3), 625–634.

Citron, M. (2010) Alzheimer's disease: strategies for disease modification. *Nat Rev Drug Discov*, 9(5), 387–398.

Çokuğraş, A.N. (2003) Butyrylcholinesterases: Structure and physiological importance. *Structure,* 28, 54-61.

Çokuğraş, A.N., and Tezcan, E.F. (1997) Amitriptyline: A potent inhibitor of butyrylcholinesterase from human serum. *General Pharmacology,* 29, 835-838.

Darvesh, S. and Hopkins, O.A. (2003) Differential distribution of butyrylcholinesterase and acetylcholinesterase in the human thalamus. *Journal of Comparative Neurology,* 463, 25-43.

De Vriese, C., Gregoire, F., Lema-Kisoka. R., Waelbroeck, M., Robberecht, P., Delporte, C. (2004) Ghrelin degradation by serum and tissue homogenates: identification of the cleavage sites. *Endocrinology*, 145(11), 4997-5005.

Duysen, E.G., Li, B., Darvesh, S. and Lockridge, O. (2007). Sensitivity of butyrylcholinesterase knockout mice to (--)-huperzine A and donepezil suggests humans with butyrylcholinesterase deficiency may not tolerate these Alzheimer's disease drugs and indicates butyrylcholinesterase function in neurotransmission. *Toxicology,* 233(1-3), 60-69.

Dvir, H., Silman, I., Harel, M., Rosenberry, T.L. and Sussman, J.L. (2010) Acetylcholinesterase: From 3D structure to function. *Chemico-Biological Interactions*, 187(1-3)**,** 10-22.

Ellman, G.L., Courtney, K.D., Andres J. v., Featherstone, R.M. (1961) A new and rapid colorimetric determination of acetylcholinesterase activity. *Biochem Pharmacol*, 7, 88-95.

Ferreira, L.G., dos Santos, R.N., Oliva, G. and Andricopulo, A.D. (2015) Molecular docking and structure-based drug design strategies. *Molecules,* 20(7), 13384-13421.

Flemmig, M. and Melzig, M.F. (2012) Serine-proteases as plasminogen activators in terms of fibrinolysis. *Journal of Pharmacy and Pharmacology* 64(8)**,** 1025-1039.

Forget, P., le Polain de Waroux, B., Wallemacq, P. and Gala, J.L. (2008) Life-threatening dextromethorphan intoxication associated with interaction with amitriptyline in a poor CYP2D6 metabolizer: a single case re-exposure study. *J Pain Symptom Manage*, 36(1), 92-96.

Francis, P.T., Palmer, A.M., Snape, M. and Wilcock, G. K. (1999) The cholinergic hypothesis of Alzheimer's disease: a review of progress. *J Neurol Neurosurg Psychiatry*, 66(2): 137–147.

Francis, P.T., Ramírez, M.J., and Lai, M.K. (2010) Neurochemical basis for symptomatic treatment of Alzheimer's disease. *Neuropharmacology,* 59(4-5), 221-229.

Gatley, S. J. (1991) Activities of the enantiomers of cocaine and some related compounds as substrates and inhibitors of plasma butyrylcholinesterase. *Biochem. Pharmaco,* 41(8), 1249–1254.

Gauthier, S. (2002) Advances in the pharmacotherapy of Alzheimer's disease. *Canadian Medical Association Journal,* 166, 616-623.

Getman, D.K., Eubanks, J.H., Camp, S., Evans, G.A. and Taylor, P. (1992) The human gene encoding acetylcholinesterase is located on the long arm of chromosome 7. *American Journal of Human Genetics,* 51(1)**,** 170-177.

Giacobini E. (2003) Cholinergic Function and Alzheimer's Disease. *Int J Geriatr Psychiatry*, 18(Suppl 1), S1–5

Giacobini, E. (2000) In Cholinesterases and Cholinesterase Inhibitor (ed. Giacobini, E.). Martin Dunitz Ltd.: London, pp. 181-226.

Giacobini, E. (2003) Butyrylcholinesterase, its Function and Inhibitors. Martin Dunitz Pub., London and New York, x+181p.

Giacobini, E. (2004) Cholinesterase inhibitors: new roles and therapeutic alternatives. *Pharmacological Research,* 50(4)**,** 433-440.

Giordano, T., Chen, D., Furukawa, K., Sambamurti, K., Brossi, A., and Lahiri, D. (2005) Selective butyrylcholinesterase inhibition elevates brain acetylcholine, augments learning and lowers Alzheimer beta-amyloid peptide in rodent. *Proceedings of the National Academy of Sciences of the United States of America*, 102(7), 17213-17218.

Girard, E., Bernard, V., Minic, J., Chatonnet, A., Krejci, E., and Molgo, J. (2007) Butyrylcholinesterase and the control of synaptic responses in acetylcholinesterase knockout mice. *Life Sci.*, 80(24-25), 2380-2385.

Gnatt, A., Loewenstein,Y., Yaron, A., Schwarz, M. and Soreq, H. (1994) Site-Directed Mutagenesis of Active Site Residues Reveals Plasticity of Human Butyrylcholinesterase in Substrate and Inhibitor Interactions. *Neurochemistry*, 62(2), 749-755.

Greig, N.H., Utsuki, T., Ingram, D.K., Wang, Y., Pepeu, G., Scali, C., Yu, Q.S., Mamczarz, J., Holloway, H.W., Giordano, T., Chen, D., Furukawa, K., Sambamurti, K., Brossi, A. and Lahiri, D.K. (2005) Selective butyrylcholinesterase inhibition elevates brain acetylcholine, augments learning and lowers Alzheimer β-amyloid peptide in rodent. *Proc Natl Acad Sci*, 102, 17213–17218.

Grosdidier, A., Zoete, V. and Michielin, O. (2007) EADock: docking of small molecules into protein active sites with a multiobjective evolutionary optimization. *J comput Chem*, 1-67(4), 1010-1025.s

Grosdidier, A., Zoete, V. and Michielin, O. (2011) SwissDock, a protein-small molecule docking web service based on EADock DSS. *Nucliec Acids Res*, 39, W270-277.

Gschwend, D.A., Good, A.C. and Kuntz, I.D. (1996) Molecular docking towards drug discovery. *J Mol Recognit.*, 9(2), 175-186.

Guedes, I.A., de Magalhães, C.S. and Dardenne, L.E. (2014) Receptor–ligand molecular docking, *Biophysical Reviews*, 6(1), 75-87.

Hitzeman, N. (2006) Cholinesterase Inhibitors for Alzheimer's disease. *Am Fam Physician*, 74(5), 747-749.

Holtzman, D.M., Morris, J.C. and Goate, A.M. (2011) Alzheimer's disease: the challenge of the second century. *Sci Transl Med*, 3(77), 77sr1.

Illanes, A. (Ed.) (2008) Enzyme biocatalysis: Principles and Applications. Chile: springer sci + Business Media B.V., pp. 116

Israel, S. and Joel, S. (2005) Acetylcholinesterase: 'Classical' and 'non-Classical' Functions and Pharmacology. *Current Opinion in Pharmacology*, 5(3), 293-302.

Jack, C.R., Petersen, R.C., Xu, Y.C., Waring, S.C., O'Brien, P.C., Tangalos, E.G. et al. (1997) Medial temporal atrophy on MRI in normal aging and very mild Alzheimer's disease. *Neurology*, 49(3), 786-794.

Jbilo, O., Bartels, C.F., Chatonnet, A., Toutant, J.P. and Lockridge, O. (1994) Tissue distribution of human acetylcholinesterase and butyrylcholinesterase messenger RNA. *Toxicon*, 32(11), 1445-1457.

Jones, M., Holland, V., and Gilmer, J.F. (2010) Isosorbide-2-benzyl carbamate-5-salicylate, a peripheral anionic site binding subnanomolar selective butyrylcholinesterase inhibitor. *Journal of Medicinal Chemistry*, 53**,** 1190-1199.

Jorgensen, A. and Hansen, V. (1976) Pharmacokinetics of amitriptyline infused intravenously in man. *Eur J Clin Pharmacol*, 10(5), 337-341.

Kaufman, S.E., Donnell, R.W., Aiken, D.C. and Magee, C. (2011) Prolonged Neuromuscular Paralysis Following Rapid-Sequence Intubation with Succinylcholine. *The Annals of Pharmacotherapy*, 45(4)**,** e21.

Kruger, R., Holzl, G., Kuss, H.J. and Schefold, L. (1986) Comparison of the metabolism of the three antidepressants amitriptyline, imipramine, and chlorimipramine in vitro in rat liver microsomes. *Psychopharmacology (Berl)*, 88(4), 505-513.

La Du, B.N., Bartells, C.F., Nogueira, C.P., Hajra, A., Lightstone, H., Van Der Spek, A. et al. (1990) Phenotypic and molecular biological analysis of human butyrylcholinesterase variants. *Clinical Biochemistry*, 23(5), 423-431.

Lamb, M.L. and Jorgensen, W.L. (1997) Computational approaches to molecular recognition. *Curr Opin Chem Biol*, 1(4), 449-457.

Lane, R.M., Potkin, S.G. and Enz, A. (2006) Targeting acetylcholinesterase and butyrylcholinesterase in dementia. *International Journal of Neuropsychopharmacology*, 9(1), 101-124.

Lee, K.J., Moussa, C.E.H., Lee, Y., Sung, Y., Howell, B.W., Turner, R.S., Pak, D.T.S. and Hoe, H.S. (2010) Beta amyloid-independent role of amyloid precursor protein in generation and maintenance of dendritic spines. *Neuroscience*, 169**,** 344-356.

Li, B., Stribley, J.A., Tieu, A., Xie, W., Schopfer, L.M., Hammond, P. *et al.* (2000) Abundant tissue butyrylcholinesterase and its possible function in the acetylcholinesterase knockout mouse. *Journal of Neurochemistry*, 75(3), 1320-1331.

Liston, D., Nielsen. J., Villalobos, A., Chapin, D., Jones, S., Hubbard, S., Shalaby, I., Ramirez, A., Nason, D. and White, W. (2004) Pharmacology of selective acetylcholinesterase inhibitors: implications for use in Alzheimer's disease. *European Journal of Pharmacology*, 486, 9-17.

Lockridge O. (2015) Review of human butyrylcholinesterase structure, function, genetic variants, history of use in the clinic, and potential therapeutic uses. *Pharmacol Ther*, 148, 34-46.

Lockridge, O. and LaDu, B. N. (1978) Comparison of atypical and usual human serum cholinesterase: purification, number of active sites, substrate affinity and turnover number. J. *Biol. Chem*, 253(6), 361-366.

Lockridge, O., Adkins, S. and La Du, B.N. (1987a) Location of disulfide bonds within the sequence of human serum cholinesterase. *The Journal of Biological Chemistry*, 262(27), 12945-12952.

Lockridge, O., Bartels, C.F., Vaughan, T.A., Wong, C.K., Norton, S.E. and Johnson, L.L. (1987b) Complete amino acid sequence of human serum cholinesterase. *The Journal of Biological Chemistry*, 262(2), 549-555.

Lockridge, O., Duysen, E. G. and Masson P. (2011) Butyrylcholinesterase: overview, structure, and function, anticholinesterase pesticides, in Anticholinesterase Pesticides: Metabolism, Neurotoxicity, and Epidemiology, eds Satoh T., Gupta R. C., editors. (Hoboken, NJ: John Wiley & Sons, Inc.), 25–41.

Lockridge, O., Mottershaw-Jackson, N., Eckerson, H., & La Du, B. N. (1980) Hydrolysis of diacetylmorphine (heroin) by human serum cholinesterase *J. Pharmacol. Exp. Ther*, 215(1), 1–8.

Lorenzo, A. and Yankner, B.A. (1994) Beta-amyloid neurotoxicity requires fibril formation and is inhibited by congo red. *Proceedings of the National Academy of Sciences of the United States of America*, 91**,** 12243-12247

Luthy, R., Bowie, J.U. and Eisenberg, D. (1992) Assessment of protein models with three-dimensional profiles. *Nature*, 356, 83-85.

Luo, W., Yu, Q., Kulkarni, S.S., Parrish, D.A., Holloway, H.W., Tweedie, D., Shafferman**,** A., Lahiri, D.K., Brossi, A. and Greig, N.H. (2006) Inhibition of Human Acetyl- and Butyrylcholinesterase by Novel Carbamates of (-)- and(+)-Tetrahydrofurobenzofuran and Methanobenzodioxepine. *J. Med. Chem*, 49(7), 2174-2185.

Maja, D. V., Ivan, O. J., Ljuba, M. M. and Branko, J. D. (2010) 4-Aryl-4-oxo-N-phenyl-2-aminylbutyramides as acetyl- and butyrylcholinesterase inhibitors. Preparation, anticholinesterase activity, docking study, and 3D structure activity relationship based on molecular interaction fields, *Bioorganic & Medicinal Chemistry*, 18, 1181–1193.

Mann, D.M. (1996) Pyramidal nerve cell loss in Alzheimer's disease. *Neurodegeneration*, 5(4), 423-427.

Manzo, R.H., Olivera, M.E., Amidon, G.C, Shah, V.P, Dressman, J.B. and Barends, D.M. (2006) Biowaiver monographs for immediate release solid oral dosage forms: Amitriptyline Hydrochloride. *J Pharm Sci*, 95(5), 966-973.

Massoud, F. and Gauthier, S. (2010) Update on the pharmacological treatment of Alzheimer's disease. Curr *Neuropharmacol*, 8(1), 69-80.

Masson, P., Froment, M.T., Bartels, C.F. and Lockridge, O. (1996) Asp7O in the peripheral anionic site of human butyrylcholinesterase, *Eur J Biochem*, 235, 36-48.

Mason, P., Carletti, E. and Nachon, F. (2009) Structure, activities and biomedical application of human butyrylcholinesterase. *Protein Pept Lett*, 16(10), 1215-1224.

Masson, P, Froment, M.T., Fortier, P.L., Visicchio, J.E., Bartels, C.F, and Lockridge, O. (1998) Butyrylcholinesterase-catalysed hydrolysis of aspirin, a negatively charged ester, and aspirin-related neutral esters. *Biochimica et Biophysica Acta (BBA) - Protein Structure and Molecular Enzymology*, 1387(1-2)**,** 41-52.

Masson, P., Xie, W., Froment, M.T., Levitsky, V., Fortier, P.L., Albaret, C. *et al.* (1999) Interaction between the peripheral site residues of human butyrylcholinesterase, D70 and Y332, in binding and hydrolysis of substrates. *Biochim. Biophys. Acta* 1433(1-2), 281–293.

McGuire, M.C., Nogueira, C.P., Bartels, C.F., Lightstone, H., Hajra, A., Vander Spek, A.F. *et al.* (1989) Identification of the structural mutation responsible for the dibucaine-resistant (atypical) variant of human serum cholinesterase. *Proceedings of the National Academy of Sciences USA,* 86(3), 953-957.

McKenna, M.T., Proctor, G.R., Young L.C. and Harvey, A.L. (1997) Novel tacrine analogues for potential use against Alzheimer's disease: potent and selective acetylcholinesterase inhibitors and 5-HT uptake inhibitors. *J Med Chem*., 24-40(22), 3516-23.

Mehndiratta, M.M., Pandey, S., and Kuntzer, T. (2011) Acetylcholinesterase inhibitor treatment for myasthenia gravis. *Cochrane Database of Systematic Reviews* 16(2)**,** CD006986.

Mesulam, M., Guillozet, A., Shaw, P and Quinn, B. (2002a) Widely spread butyrylcholinesterase can hydrolyze acetylcholine in the normal and Alzheimer brain. *Neurobiology of Disease*, 9(1), 88-93.

Mesulam, M.M., Guillozet, A., Shaw, P., Levey, A., Duysen, E.G. and Lockridge, O. (2002b) Acetylcholinesterase knockouts establish central cholinergic pathways and can use butyrylcholinesterase to hydrolyse acetylcholine. *The Journal of Neuroscience,* 110(4), 627-639.

Mico, J.A., Ardid, D., Berrocoso, E. and Eschalier, A. (2006) Antidepressants and pain. *Trends Pharmacol Sci*, 27(7), 348-354.

Mucke, L. (2009) Neuroscience: Alzheimer's disease. *Nature*, 461(7266), 895–897

Mukesh, B. and Rakesh, K. (2011) Molecular docking: a review. *IJRAP*, 2(6), 1746-1751.

Muller, T.C., Rocha, J.B.T., Morsch, V.M., Neis, R.T. and Schetinger, M.R.C. (2002) Antidepressants inhibit human acetylcholinesterase and butyrylcholinesterase activity. *Biochim Biophys Acta*, 1587(1), 92–98.

Mumford, H., Docx, C.J., Price, M.E., Green, A.C., Tattersall, J.E. and Armstrong, S.J. (2013) Human plasma-derived BuChE as a stoichiometric bioscavenger for treatment of nerve agent poisoning. *Chemico-Biological Interactions***,** 203, 160-166.

Munoz-Muriedas J., Lopez J.M., Orozco, M. and Luque, F.J. (2004) Molecular modelling approaches to the design of acetylcholinesterase inhibitors: new challenges for the treatment of Alzheimer's disease. *Curr Pharm Des,* 10(25), 3131–3140.

Nachon, F., Nicolet, Y., Viguié, N., Masson, P., Fontecilla-Camps, J. and Lockridge, O. (2002) Engineering of a monomeric and low-glycosylated form of human butyrylcholinesterase: expression, purification, characterization and crystallization. *European Journal of Biochemistry,* 269(2)**,** 630-637.

Nawaz, S.A., Ayaz, M., Brandt, W., Wessjohann, L.A. and Westermann, B. (2011) Cation-π and π-π stacking interactions allow selective inhibition of butyrylcholinesterase

by modified quinine and cinchonidine alkaloids. *Biochemical and Biophysical Research Communications,* 404**,** 935-940.

Newberry, D.L., Bass, S.N. and Mbanefo, C.O. (1997) A fluconazole/amitriptyline drug interaction in three male adults. *Clin Infect Dis,* 24(2), 270-271.

Ngamelue, M., Homma, K., Lockridge, O. and Asojo, O. (2007) Crystallization and X-ray structure of full-length recombinant human butyrylcholinesterase. *Acta Crystallographica Section F: Structural Biology and Crystallization Communications,* 63**,** 723-7.

Nicolet, Y., Lockridge, O., Masson, P., Fontecilla-Camps, J.C. and Nachon, F. (2003) Crystal structure of human butyrylcholinesterase and of its complexes with substrate and products. *The Journal of Biological Chemistry,* 278(42), 4114-41147

Nielsen, M., Lundegaard, C., Lund, O. and Petersen, T.N. (2010) CPHmodels-3.0--Remote homology modeling using structure guided sequence profiles. *Nucleic Acids Research*, 38, W576-581.

Nogueira, C.P., Bartels, C.F., McGuire, M.C., Adkins, S., Lubrano, T., Rubinstein, H.M. *et al.* (1992) Identification of two different point mutations associated with fluoride-resistance phenotype for human butyrylcholinesterase. *Am J Hum Genet*, 51(4), 82-88.

Norfray, J.F. and Provenzale, J.M. (2004) Alzheimer's disease: Neuropathologic findings and recent advances in imaging. *AJR Am J Roentgenol*, 182(1), 3-13

Nunes-Tavares, N., Matta, A.N., Silva, C.M.B., Arau´ jo, G.M.N., Louro, S.R.W., Hasso´n-Voloch, A. (2002) Inhibition of acetylcholinesterase from Electrophorus electricus by tricyclic antidepressants. *Int J Biochem Cell Biol*, 34(9), 1071–1079.

Ozer, I. and Kucukkilinc, T. (2005) Inhibition of human plasma cholinesterase by malachite green and related triarylmethane dyes: Mechanistic implications. *Archives of Biochemistry and Biophysics,* 440, 118-122.

Perkinson, E., Ruckart, R. and Davanzo, J. P. (1969) Pharmacological and biochemical studies in isolation induce fighting mice. *Proc soc Ex Biol Med*, 131(2), 685-689.

Podoly, E., Shaley, D.E., Shenhar-Tsarfaty, S., Bennett, E.R., Assayag, E.B., Wilgus, H., Livnah, O. and Soreq, H. (2009) The butyrylcholinesterase K variant confers structurally derived risks for Alzheimer pathology. *J Biol Chem*, 284(25), 17170–17179.

Pohanka, M. (2011) Cholinesterases, a target of pharmacology and toxicology. *Biomedical papers of the Medical Faculty of the University Palacký, Olomouc, Czech Republic*, 155(3), 219-229.

Pohanka, M. (2014) Inhibitors of acetylcholinesterase and butyrylcholinesterase meet immunity. *Int J Mol Sci*, 15(6), 9809–9825.

Qian, Z.M. and Ke, Y. (2014) Huperizine A: is it an effective disease modifying drug for Alzheimer's disease? *Frontiers in Aging neuroscience*, 6: 216. doi:10.3389/fnagi.2014.00216.

Querfurth, H.W. and LaFerla, F.M. (2010) Alzheimer's disease. *N Engl J Med*, 362(4), 329-344.

Radic, Z., Pickering, N.A., Vellom, D.C., Camp, S. and Taylor, P. (1993) Amino acid residues controlling acetylcholinesterase and butyrylcholinesterase specificity. *Biochemistry*, 32(1), 12074–12084.

Raveh, L., Grauver, E., Grunwald, J., Cohen, E. and Ashani, Y. (1997) The stoichiometry of protection against soman and VX toxicity in monkeys pretreated with human butyrylcholinesterase. *Toxicol. Appl. Pharm*, 145(1), 43-53.

Rees, T., Hammond, P. I., Soreq, H., Younkin, S., Brimijoin, S. (2003) Acetylcholinesterase promotes β-amyloid plaques in cerebral cortex. *Neurobiol. Aging*, 24(6), 777–787.

Reyes, A.E., Perez, D.R., Alvarez, A., Garrido, J., Gentry, M.K., Doctor B.P. and Inestrosa, N.C. (1997) A monoclonal antibody against acetylcholinesterase inhibit the

formation of amyloid fibrils induced by the enzyme. *Biochem. Biophys. Res. Commun*., 232(3), 652-655.

Rollins, D.E., Alvan, G., Bertilsson, L., Gillette, J.R., Mellstrom, B., Sjoqvist, F. and Traskman, L. (1980) Interindividual differences in amitriptyline demethylation. *Clin Pharmacol Ther*, 28(1), 121-129.

Rubinstein, H.M., Lubrano, T., and La Du B.N. (1992) DNA mutation associated with the human butyrylcholinesterase K-variant and its linkage to the atypical variant mutation and other polymorphic sites. *Am J Hum Genet*, 50(5), 1086–1103.

Salentin, S., Schreiber, S., Haupt, V.J., Adasme, M.F. and Schroeder, M. (2015) PLIP: fully automated protein-ligand interaction profiler. *Nucl. Acids Res.*, 43 (W1), W443-W447.

Saxena, A., Redman, A.M., Jiang, X., Lockridge, O. and Doctor, B.P. (1997) Differences in active site gorge dimensions of cholinesterases revealed by binding of inhibitors to human butyrylcholinesterase, *Biochemistry*, 36(48), 14642-14651.

Schein, K. and Smith, S.E. (1978) Structure-activity relationship for the anticholinoceptor action of tricyclic antidepressants. *Br. J. Pharmac*, 62(4), 567-571.

Schmider, J., Greenblatt, D. J., Von Moltke, L. L., Harmatz, J. S. and Shader, R.I. (1995) N-Demethylation of amitriptyline *in vitro:* role of cytochrome P-4503A (CYP 3A) isoforms and effect of metabolic inhibitor. J. Pharmac. Exp. Ther., 275(2), 592-597.

Schulz, P., Turner-Tamiyasu, K., Smith, G., Giacomini, K.M. and Blaschke, T.F. (1983) Amitriptyline disposition in young and elderly normal men. *Clin Pharmacol Ther*, 33(3), 360-366.

Segel, I.R. (1975) *Enzyme Kinetics*, New York: John Wiley and Sons Ins.

Shaikh, S., Verma, A., Siddiqui, S., Ahmad, S.S., Rizvi, S.M., Shakil, S., Biswas, D., Singh, D., Siddiqui, M.H., Shakil, S., Tabrez, S. and Kamal, M.A. (2014) Current

acetylcholinesterase-inhibitors: A neuroinformatics perspective. *CNS Neurol Disord Drug Targets*, 13(3), 391–401.

Shoichet, B.K., McGovern, S.L., Wei, B. and Irwin, J.J. (2002) Lead discovery using molecular docking. *Curr Opin Chem Biol*, 6(4), 439-446.

Silk, E., King, J. and Whittaker, M. (1979) Assay of cholinesterase in clinical chemistry. *Anal. Clin. Biochem*., 16, 57-75.

Silver, A. (1974) The biology of cholinesterases. Amsterdam: Elsevier

Sim, A. (1999) Rivastigmine: a review. *Hosp. Med*. 60(10), 731–735.

Soreq, H. and Seidman, S. (2001) Acetylcholinesterase — new roles for an old actor. *Nature Rev. Neurosci.*, 2(4), 294–302

Steimer, W., Zopf, K., Von Amelunxen, S., Pfeiffer, H., Bachofer, J., Popp, J., Messner B., Kissling, W. and Leucht, S. (2005) Amitriptyline or not, that is the question: pharmacogenetic testing of CYP2D6 and CYP2C19 identifies patients with low or high risk for side effects in amitriptyline therapy. *Clin Chem*, 51(2), 376-385

The PyMOL Molecular Graphics System, Schrödinger LCC, open source v.1.2x. http://www.pymol.org

Toda, N., Kaneko, T. and Kogen, H. (2010) Development of an efficient therapeutic agent for Alzheimer's disease: design and synthesis of dual inhibitors of acetylcholinesterase and serotonin transporter. *Chem Pharm Bull*, 58, 273–287.

Tunek, A. and Svensson, L.A. (1988) Bambuterol, a carbamate ester prodrug of terbutaline, as inhibitor of cholinesterases in human blood. *Drug Metabolism and Disposition*, 16(5), 759-764.

Turner, P.R., O'Connor, K., Tate, W.P. and Abraham, W.C. (2003) Roles of amyloid precursor protein and its fragments in regulating neural activity, plasticity and memory. *Progress in Neurobiology*, 70**,** 1-32.

Van der Spek, A.F., Lockridge, O. and La Du, B.N. (1992) Identification of two different point mutations associated with the fluoride-resistant phenotype for human butyrylcholinesterase. *Am J Hum Genet*, 51(4), 821-828.

Vellom, D. C., Radiz, Z., Li, Y., Pickering, N.A., Camp, S. and Taylor P. (1993) Amino acid residues controlling acetylcholinesterase and butyrylcholinesterase specificity. *Biochemistry,* 32(1), 12–17.

Venkatakrishnan, K., Greenblatt, D.J., von Moltke, L.L., et al. (1998) Five distinct human cytochromes mediate amitriptyline N-demethylation in vitro: dominance of CYP 2C19 and 3A4. *J Clin Pharmacol*, 38(2), 112-121.

Verdu, B., Decosterd, I., Buclin, T., Stiefel, F. and Berney, A. (2008) Antidepressants for the treatment of chronic pain. *Drugs*, 68(18), 2611-2632.

Whitcomb, D.C. and Lowe, M.E. (2007) Human pancreatic digestive enzymes. *Digestive Diseases and Sciences*, 52(1), 1-17.

WHO (2016) Factsheets fs362. Ten facts about dementia. World Health Organization

Xu, Z., Yao Swei, Y., Zhou, J., Zhang, L., Wang, C. and Guo, Y. (2008) Monitoring Enzyme Reaction and Screening of Inhibitors of Acetylcholinesterase by Quantitative Matrix-Assisted Laser Desorption/Ionization Fourier Transform Mass Spectrometry. *Journal of the American Society for Mass Spectrometry,* 19(12), 1849-1855.

Xue, L., Ko, M-C., Tong, M., Yang, W., Hou, S., Fang, L. *et al.* (2011) Design, Preparation, and Characterization of High-Activity Mutants of Human Butyrylcholinesterase Specific for Detoxification of Cocaine, *Molecular Pharmacology* 79(2), 290-297.

Zhang, J., Chen, S., Ralph, E.C., Dwyer, M. and Cashman, J.R. (2012) Identification of Human Butyrylcholinesterase Organophosphate-Resistant Variants through a Novel Mammalian Enzyme Functional Screen. *Journal of Pharmacology and Experimental Therapeutics,* 343(3)**,** 673-682.